THE UNIVERSITY OF MICHIGAN

COLLEGE OF ENGINEERING
Department of Electrical Engineering
Space Physics Research Laboratory

Sounding Rocket Instrumentation and Flight Report

NASA 18.78 GA MODEL A PLANETARY MASS SPECTROMETER TEST FLIGHT

Prepared on behalf of the project by

D. F. Crosby
D. L. Jones

ORA Project 02681

under contract with:

NATIONAL AERONAUTICS AND SPACE ADMINISTRATION
GODDARD SPACE FLIGHT CENTER
CONTRACT NO. NAS5-11128
GREENBELT, MARYLAND

administered through:

OFFICE OF RESEARCH ADMINISTRATION ANN ARBOR

January 1970

ensn

UMR0936

TABLE OF CONTENTS

TABLE OF CONTENTS (Concluded)

ACKNOWLEDGMENTS

The Model A planetary mass spectrometer test flight was conducted under Contract NAS5-11128 as a cooperative undertaking of Goddard Space Flight Center's Laboratory for Atmospheric and Biological Sciences and the Space Physics Research Laboratory of The University of Michigan. Obviously a complete listing of those contributing to the success of the flight would be too lengthy to include here; however, personnel with specific responsibilities are listed below.

Goddard Space Flight Center

J. E. Cooley	Project Scientist
H. Dewey	Mechanical Engineer
D. W. Grimes	Project Manager
D. N. Harpold	Experimenter
N. W. Spencer	Project Director

Space Physics Research Laboratory
(The University of Michigan)

G. R. Carignan	Laboratory Director
J. R. Cutler	Electrical Engineer
C. E. Hubler	Payload Technician
R. G. Kimble	Telemetry Technician
R. W. Simmons	Data Processing Manager

Gas Dynamics Laboratories
(The University of Michigan)

D. E. Geister
D. R. Glass

LIST OF FIGURES

LIST OF FIGURES (Continued)

LIST OF FIGURES (Concluded)

1. INTRODUCTION

The Model A Planetary Test Flight was designed as the first in a series of test flights to qualify a quadrupole mass spectrometer for high-pressure neutral constituent measurements on future planetary exploratory missions. The spectrometer, which was designed and built by the Laboratory for Atmospheric and Biological Sciences at Goddard Space Flight Center (GSFC), was the first test of a sterilized mass spectrometer electronics system in a flight environment. The spectrometer employed a unique pressure reduction device at its inlet orifice to permit measurements to be made at higher pressures than those measured by previous earth atmosphere devices.

The measurement region for this mission was chosen to be 30 to 60 km on the basis that the ambient pressure profile in this portion of the earth's atmosphere corresponds to a region in the Martian atmosphere from 0 to 25 km. The nose cone design incorporated an atmospheric sample inlet system which provided a tolerable pressure and temperature profile at the mass spectrometer inlet orifice for this region.

The payload contained temperature and pressure sensors mounted within the nose cone for the purpose of verifying the inlet system design. In addition to the control and telemetry circuitry, the payload also contained a magnetometer to provide aspect information, a thrust axis accelerometer to monitor rocket performance, and a pyrotechnically activated breakoff device to open the spectrometer to the atmosphere at the desired point in the trajectory.

The present report describes the payload instrumentation and the sample inlet system design in detail and provides flight trajectory, temperature, and pressure data. The mass spectrometer data are being processed by GSFC and are not presented here.

2. GENERAL FLIGHT INFORMATION

The general flight information for NASA 18.78 GA is listed below. The table gives the flight times and altitudes of significant events which occurred during the flight. These parameters were obtained from the flight records and radar trajectory information.

Launch Date:	21 August 1969
Launch Time:	14:09 GMT; 10:09 AM, EDT
Location:	Wallops Island, Virginia
	Latitude: 37°50'14.915" N
	Longitude: 79°29'01.693" W

NASA 18.78 GA TABLE OF EVENTS

Event	Flight Time (sec)	Altitude (km)
Lift-off	0	0
Nike Burnout	3.5	1.7
Tomahawk Ignition	11.6	6.2
Auto Filament Switch Enable	19.0 (est.)	14.0 (est.)
Tomahawk Burnout	21.0	17.7
Mass Spectrometer Inlet Opening	24.5	24.8
Enter Measurement Region	27.2	30.0
Exit Measurement Region	43.4	60.0
Apogee	236.0	227.4
L. O. S.	460.0	-----

3. LAUNCH VEHICLE

The NASA 18.78 GA launch vehicle was a Nike-Tomahawk two-stage, solid propellant, fin-stabilized, unguided sounding rocket. The first stage was a standard Nike (M5) rocket motor with a nominal 3.5 sec burning time. The second stage was a Thiokol Tomahawk (TE 416) rocket motor with a zero delay pyrogen igniter and a nominal burning time of 9 sec.

The Nike used Aerolab type fins canted 12 min to produce a nominal 1.2 rps roll rate at burnout. The Tomahawk used Astro-Met type fins canted 20 min to produce a nominal 6 rps roll rate at burnout. At Nike burnout, the two stages drag-separated and the second stage Tomahawk coasted until T+12 sec, at which time the second stage igniter fired by means of an on board timer and battery pack located in the firing and despin module (FDM). The Tomahawk and payload were not despun, and the coning angle and angle of attack were thereby minimized.

The launch vehicle, illustrated in Figures 1 and 2, performed satisfactorily and boosted the payload to an apogee of 227.4 km, 236.0 sec after lift-off.

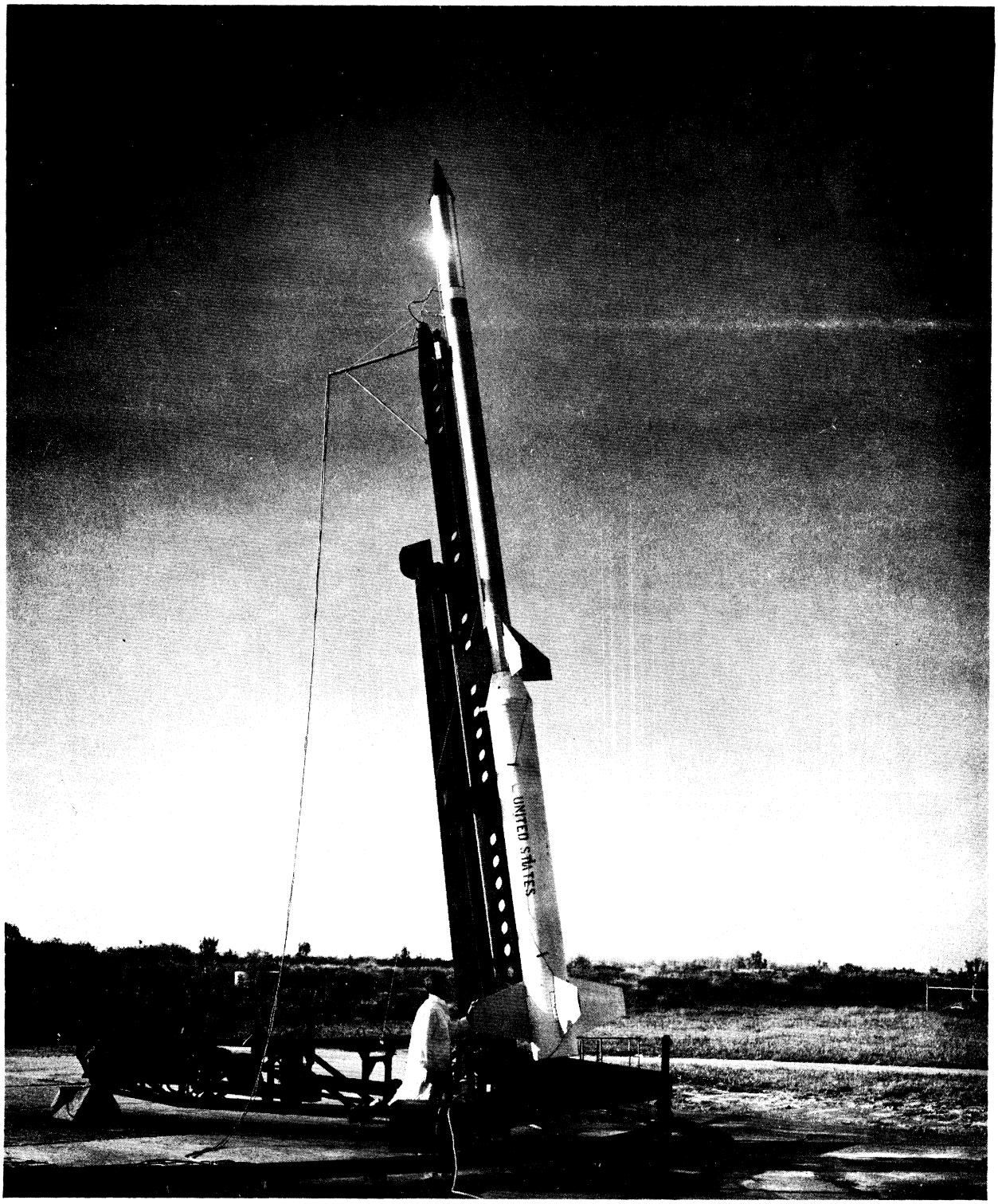

Figure 1. Rocket elevated for launch.

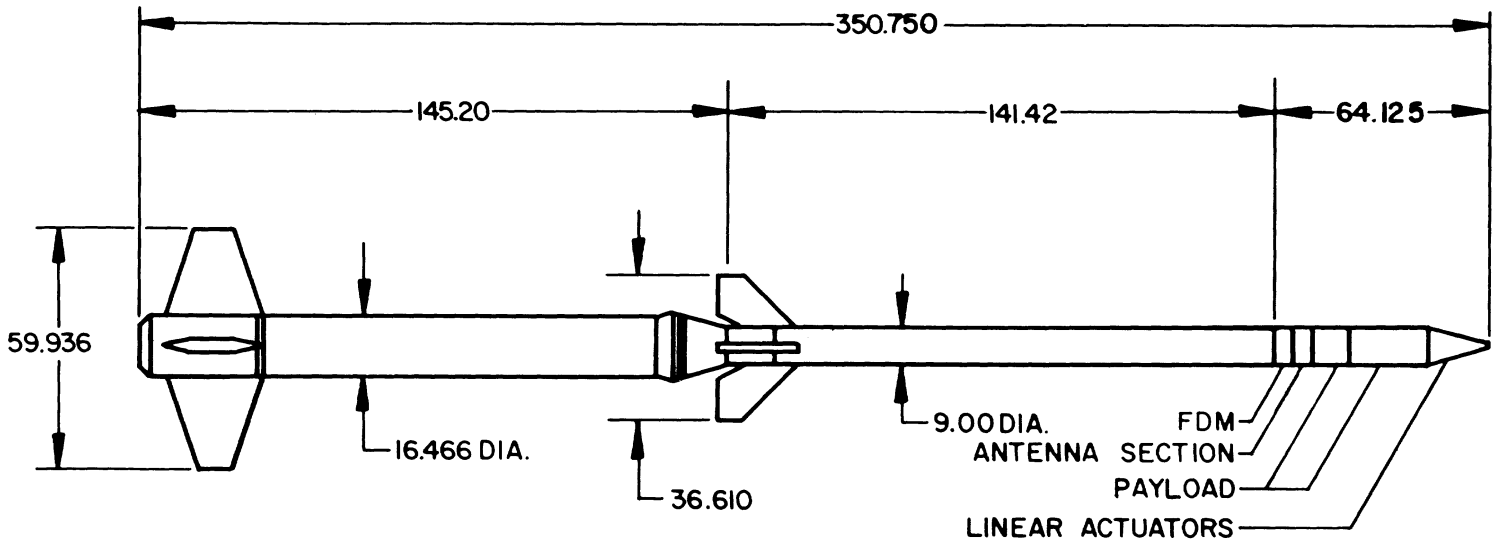

VEHICLE WEIGHT

BOOSTER	1325 LBS.
TOMAHAWK	537
	1862 LBS. TOTAL

PAYLOAD WEIGHT 18.78 GA

FDM	11.8 LBS.
ANTENNA SECTION	17.7
EXPERIMENTS & CONTROL	177.4
	206.9 LBS. TOTAL

NIKE-TOMAHAWK

Figure 2. Rocket and payload.

4. PAYLOAD

Figure 3 shows the payload configuration for NASA 18.78 GA. Figure 4 is an assembly drawing of the payload excluding the antenna section and the fire and despin module which were furnished by GSFC. The nose cone section, quadrupole mass spectrometer section, and the control and telemetry section are discussed in this part of the report. Figure 5 is a block diagram of the complete payload.

At T+24.5 sec the timer provided a signal to fire the redundant Conax linear actuators (-8 on Figure 4) which fractured the ceramic of the breakoff unit (-4 of Figure 4), thus exposing the spectrometer inlet orifice to the atmosphere. The temperature sensor (-10R of Figure 4) and the pressure sensor (-9R of Figure 4) provided temperature and pressure data within the sample inlet system nose cone cavity from lift-off to loss of telemetry signal.

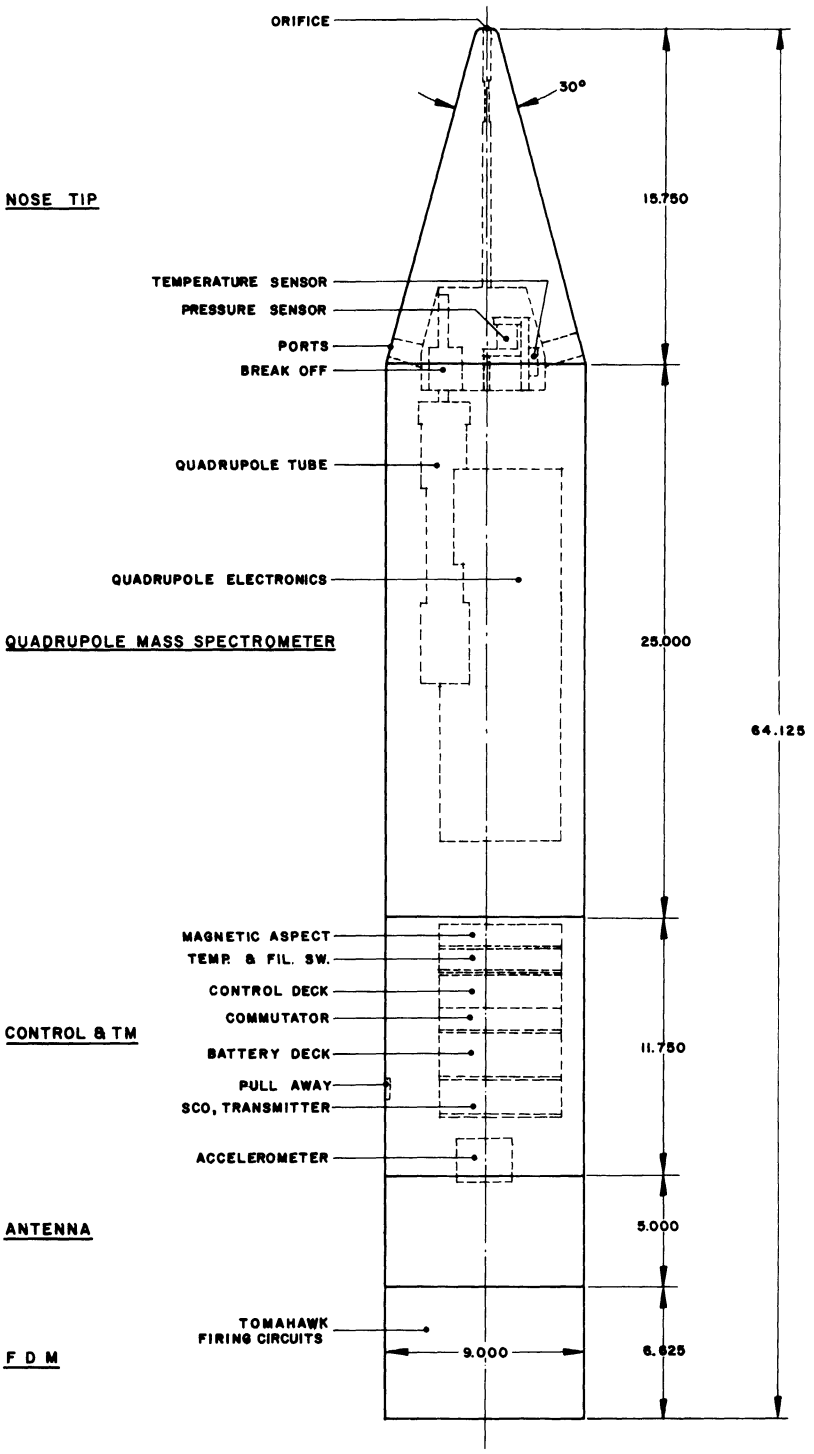

NAME	WEIGHT	C.G. FROM TIP
PROBE	177.4 lbs	
FDM	11.8 lbs	
ANTENNA	17.7 lbs	
TOTAL	206.9 lbs	26.655"

MISC. NOTES:

ROCKET NO.	18.78 GA
LAUNCH RANGE NO.	WALLOPS IS., VA.
TYPE OF ROCKET	NIKE-TOMAHAWK
DATE OF LAUNCH	8-21-69
LOCATION	WALLOPS ISLAND
TIME	10:09 EDT 14:09 GMT
ALTITUDE	227.4 KM
RESULTS ROCKET AND PAYLOAD PERFORMED AS EXPECTED.	

Figure 3. Payload configuration.

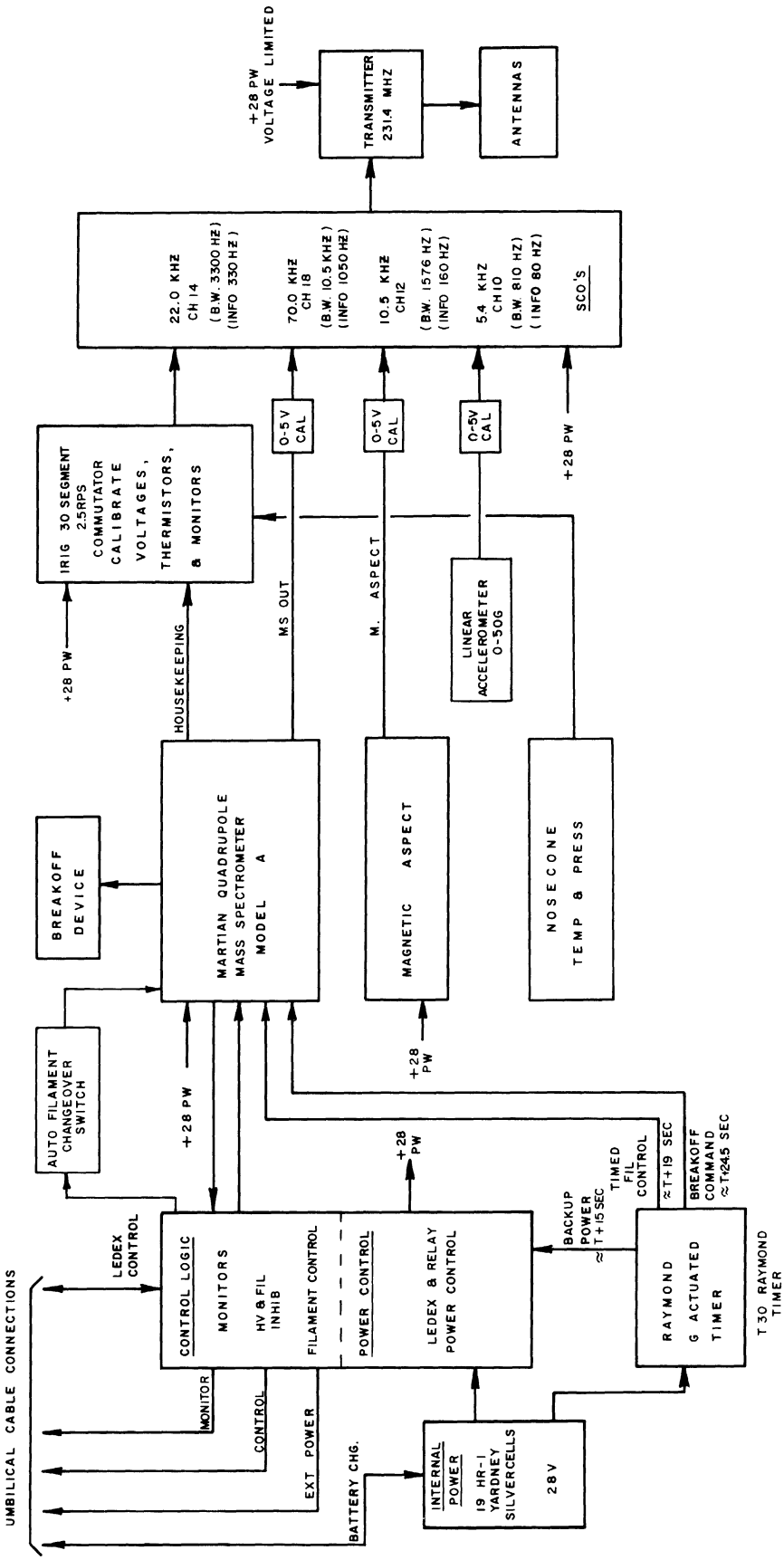

Figure 5. Payload block diagram.

4.1. NOSE CONE AND INLET SYSTEM

The design of the nose cone and sample inlet system was based on the principle of providing an environment in the earth's atmosphere which would be similar to that encountered by a high velocity entry into the atmosphere of Mars. The design was limited by the performance characteristics of the Nike-Tomahawk launch vehicle in that the high velocity (15,000-20,000 ft/sec) and resulting high stagnation conditions of a Martian entry could not be simulated. Also, since the Tomahawk stage did not include an attitude control system, the mission was dependent upon an upleg measurement. As it turned out, however, the payload and attached Tomahawk stage stabilized very soon after encountering the aerodynamic drag region on the downleg, and consequently some usable data were obtained on the reentry portion of the trajectory.

The measurement region was chosen to be 30 to 60 km on the basis that the ambient pressure of this portion of the earth's atmosphere is close to that in the expected Martian atmosphere from 0 to 25 km. The design objectives of the nose cone were to transport a sample of the atmosphere to the mass spectrometer inlet orifice as rapidly as possible and at a temperature and pressure that would not affect the pressure reduction device at the inlet orifice. The pressure reduction device is a sintered stainless steel leak that provides molecular flow into the mass spectrometer, if the pressure external to the leak is not too high. The leak used in this experiment required that the pressure in the sample chamber be below 100 mmHg. The leak conductance is also dependent, to a lesser extent, on its temperature. The nose cone and the inlet system were designed to maintain the maximum pressure in the sample chamber below 100 mmHg, and to reduce the temperature of the incoming gas to a level such that the total heat input to the leak did not raise its temperature more than 50°F. (More than a 50°F rise results in a change in leak conductance.)

On the basis of three requirements, solid stainless steel was selected for the nose cone:

(1) capability to withstand the high stagnation temperatures without appreciable chemical reaction with the incoming gas sample,

(2) capability to act as a heat sink to the gas sample,

(3) capability to insulate the incoming gas sample from aerodynamic heating of the conewall.

Stainless steel is the least reactive of the readily available metals capable of withstanding the high stagnation temperatures. Copper, or a metal of similar heat conductivity, would have been the obvious choice for a heat sink but these metals are all very reactive and oxidize readily at high temperatures. The conductivity of stainless steel is high enough to reduce the gas temperature to the required level. The critical flow section of the inlet system was recessed (Figure 6) 2.5 in. to reduce the amount of aerodynamic heating input to a mini-

mum. Because of the large mass and relatively low conductivity of the metal surrounding this section and because the time duration in the aerodynamic drag region was quite short, the external heat contribution from conewall heating was very low. During flight, the gas temperature was monitored by using a platinum wire temperature sensor built by Rosemount Engineering Corporation. This sensor was mounted near one of the exhaust ports to insure that it would be in the flow stream where the time response would be a maximum. Figures 38(a) and 38(b) show theoretical versus measured altitude profiles of temperature.

The pressure reduction was accomplished by using a critical flow section (Figure 6) which limits the flow rate by choking the flow and large expansion volume of the sample chamber. The exhaust ports were designed to be large enough with respect to the small diameter of the choking section so that the only restriction to exiting flow would be the external conewall pressure. A pressure transducer built by Spartan Southwest Engineering was used to measure the static pressure in the chamber. The transducer was mounted so that the pressure was monitored near the top of the chamber where purely static conditions most likely prevail. Figures 39(a) and 39(b) shows theoretical versus measured altitude profiles of pressure.

To verify the calculations of pressure and temperature, wind tunnel tests were run in which a 1/5 scale model of the nose cone was used (see Appendix). Another objective of the tests was to determine whether there would be a positive flow rate throughout the measurement region. Since the pressure measured in the chamber was always higher than the conewall pressure, a positive flow rate was indicated. The gas temperature coming into the sample chamber was measured and indicated that the temperature in the sample chamber was about 20% of the free-stream stagnation temperature. This agrees closely with the theoretical temperatures in Figures 38(a) and 38(b).

Good data were received from both temperature and pressure sensors throughout the measurement region and close agreement was shown between the theoretical and the laboratory data.

4.2. SPECTROMETER SECTION

The spectrometer section assembly, shown in Figure 4, contains the mass spectrometer electronics (-2R), the quadrupole analyzer tube (-6R), the breakoff device (-4), the linear actuator assemblies (-8), the pressure sensor (-6), and the temperature sensor (-10R). Each of the above-mentioned components is discussed below.

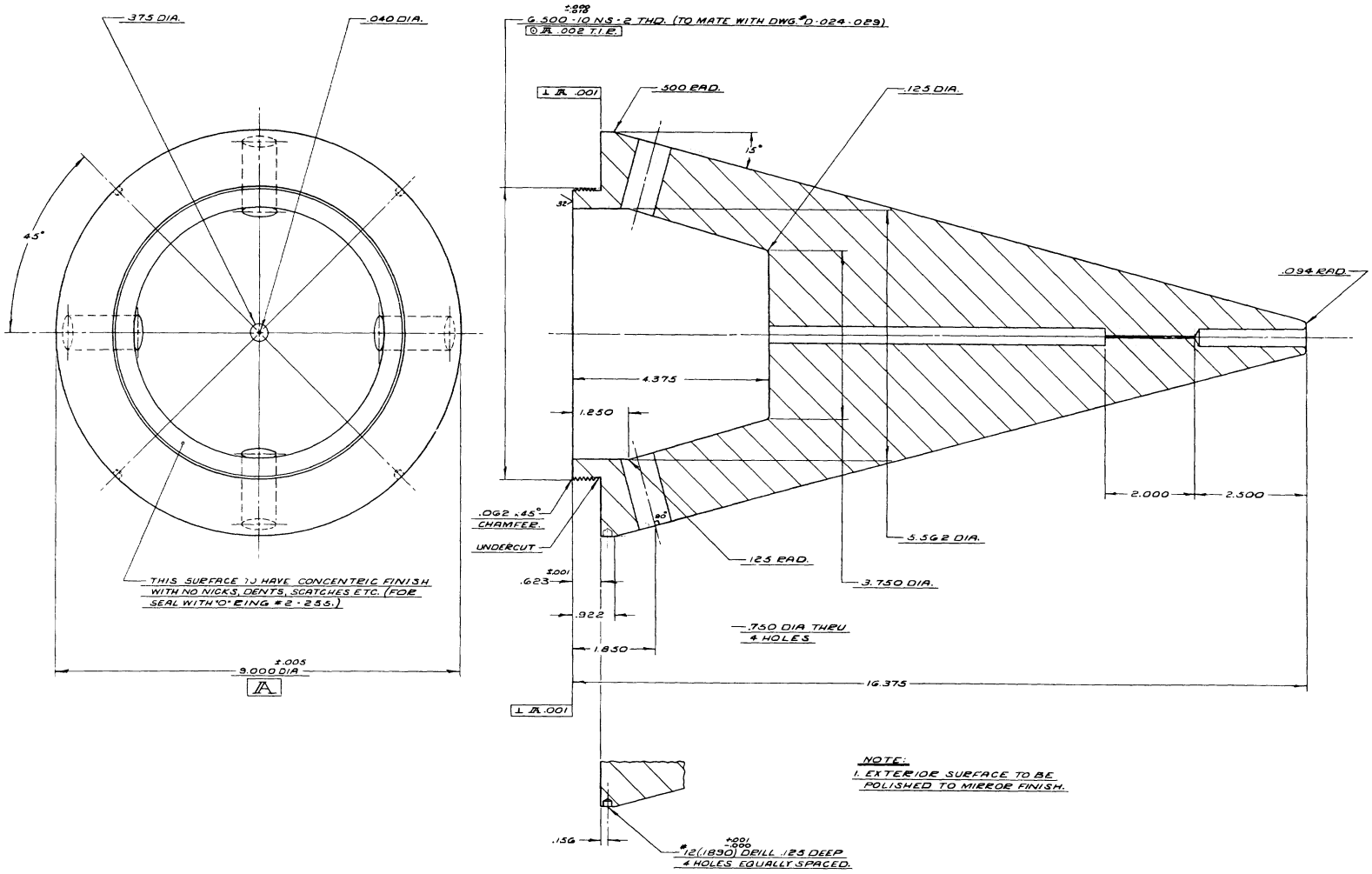

Figure 6. Nose cone.

4.2.1. Mass Spectrometer Electronics and Quadrupole Analyzer Tube

The mass spectrometer system (Kerne, Deskevich, and Elder, 1968; Consultants and Designers, Inc., 1968), consisting of the electronics and the analyzer tube, was supplied by GSFC and is described only briefly here.

The mass spectrometer system is designed to measure the neutral atmospheric constituents with masses between 10 and 50 amu. The spectrometer is continuously tunable and scans through one complete cycle every 2 sec. The spectrometer output, an analog voltage proportional to the relative abundance of the mass number to which it is tuned, is supplied to the payload telemetry unit. Several housekeeping voltages are also monitored to assure proper spectrometer flight operation.

4.2.2. Breakoff Device

The breakoff device assembly drawing is shown in Figure 7. This device provided a seal for the mass spectrometer inlet orifice until the spectrometer was in the desired region of the atmosphere. When the desired altitude was reached (at T+24.5 sec), two linear actuators were fired, which fractured the ceramic at the scored line about its circumference. The upper portion of the breakoff device is captured by a spring-loaded retaining device and the spectrometer was opened to the atmosphere.

4.2.3. Linear Actuator Assembly

The linear actuator assembly is shown in Figure 8 and the actuator itself is shown in Figure 9. The actuator housing was a safety precaution which insured that any gases escaping from the actuator itself during its activation would not contaminate the mass spectrometer measurement. Two actuator assemblies were used for the sake of reliability.

4.2.4. Pressure Sensor

The pressure sensor and its interface to the payload are shown in Figure 10. The final calibration curve for this 0-1 psia sensor is shown in Figure 11. The pressure sensor was used to provide verification data on the sample inlet system of the nose cone.

4.2.5. Temperature Sensor

The temperature sensor is shown in Figure 12 and its final calibration tabulation in Figure 13. The temperature sensor was used to provide data to verify the design parameters of the nose cone sample inlet system.

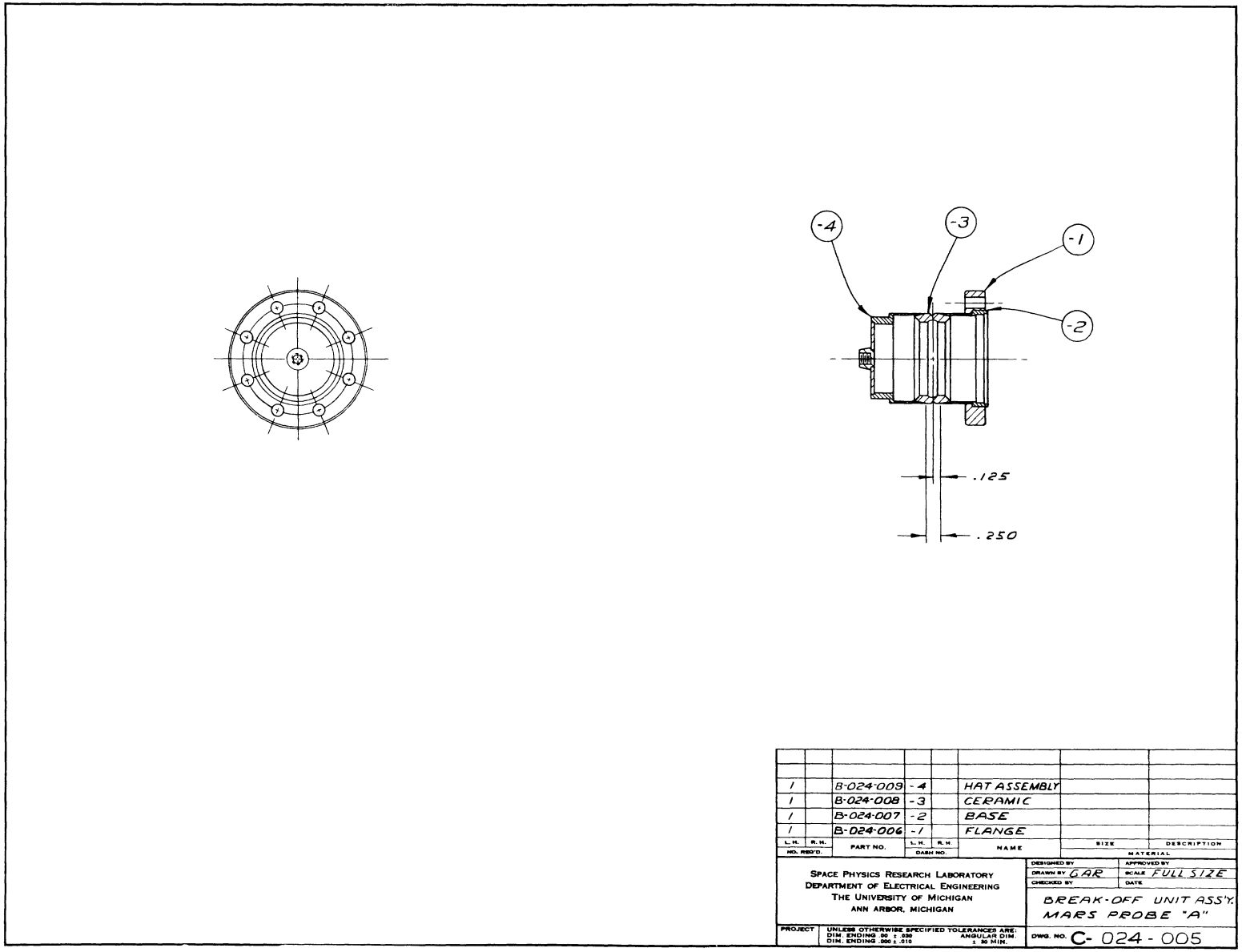

1		B-024-009	-4		HAT ASSEMBLY			
1		B-024-008	-3		CERAMIC			
1		B-024-007	-2		BASE			
1		B-024-006	-1		FLANGE			
L.H.	R.H.	PART NO.	L.H.	R.H.	NAME	SIZE	DESCRIPTION	
NO. REQ'D.			DASH NO.			MATERIAL		

SPACE PHYSICS RESEARCH LABORATORY
DEPARTMENT OF ELECTRICAL ENGINEERING
THE UNIVERSITY OF MICHIGAN
ANN ARBOR, MICHIGAN

DESIGNED BY
DRAWN BY GAR
CHECKED BY
APPROVED BY
SCALE FULL SIZE
DATE

BREAK-OFF UNIT ASS'Y.
MARS PROBE "A"

PROJECT

UNLESS OTHERWISE SPECIFIED TOLERANCES ARE:
DIM. ENDING .00 ± .030
DIM. ENDING .000 ± .010
ANGULAR DIM. ± 30 MIN.

DWG. NO. C- 024 - 005

Figure 7. Breakoff device assembly.

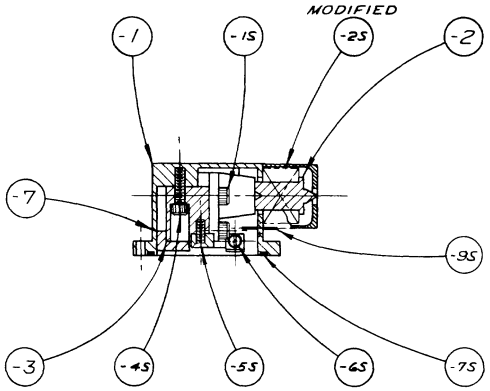

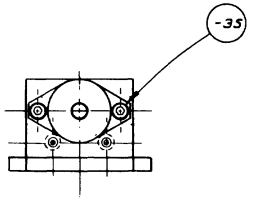

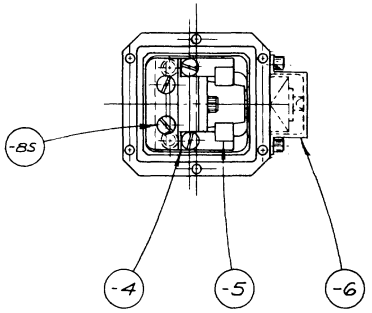

2			-9S		FEED THRU		
2		STANDARD	-8S		FLAT HD. SCR.	#4-40NC-2×.312	ST'N. ST.
1		PARKER SEAL #231	-7S		"O" RING	1¾" × 1⅞" × 1/16"	VITON 77-545
2		STANDARD	-6S		ROUND HD. SCR.	#4-40NC-2×.125	BRASS
2		STANDARD	-5S		FLAT HD. SCR.	#4-40NC-2×.375	BRASS
2		STANDARD	-4S		SOC. HD. CAP SCR.	#6-32NC-2×.500	PARKERIZED
2		STANDARD	-3S		SOC. HD. CAP SCR.	#4-40NC-2×.500	PARKERIZED
1		GARDNER BELLOW CORP. #S1800B	-2S		STOCK BELLOWS (MOD) TO	.500 ACTIVE LG. .625 TOTAL LG.	321 ST'N. ST.
3		STANDARD	-1S		SOC. HD. CAP SCR.	#6-32NC-2×.375	PARKERIZED
1		A-024-018	-7		SPACER		
1		B-024-026	-6		RETAINER		
2		A-024-017	-5		CONTACT		
1	1	A-024-016	-4		INSULATOR		
1		B-024-015	-3		ADAPTER		
1		B-024-019	-2		PLUNGER		
1		C-024-014	-1		BODY		
L.H.	R.H.	PART NO.	L.H.	R.H.	NAME	SIZE	DESCRIPTION
NO. REQ'D.			DASH NO.			MATERIAL	

SPACE PHYSICS RESEARCH LABORATORY
DEPARTMENT OF ELECTRICAL ENGINEERING
THE UNIVERSITY OF MICHIGAN
ANN ARBOR, MICHIGAN

DESIGNED BY | APPROVED BY
DRAWN BY GAR | SCALE FULL SIZE
CHECKED BY | DATE 8-7-68

ACTUATOR SEALED HOUSING ASS'Y.
MARS PROBE MOD. "A"

PROJECT

UNLESS OTHERWISE SPECIFIED TOLERANCES ARE:
DIM. ENDING .00 ± .030
DIM. ENDING .000 ± .010
ANGULAR DIM. ± 30 MIN.

DWG. NO. C-024-013

Figure 8. Linear actuator assembly.

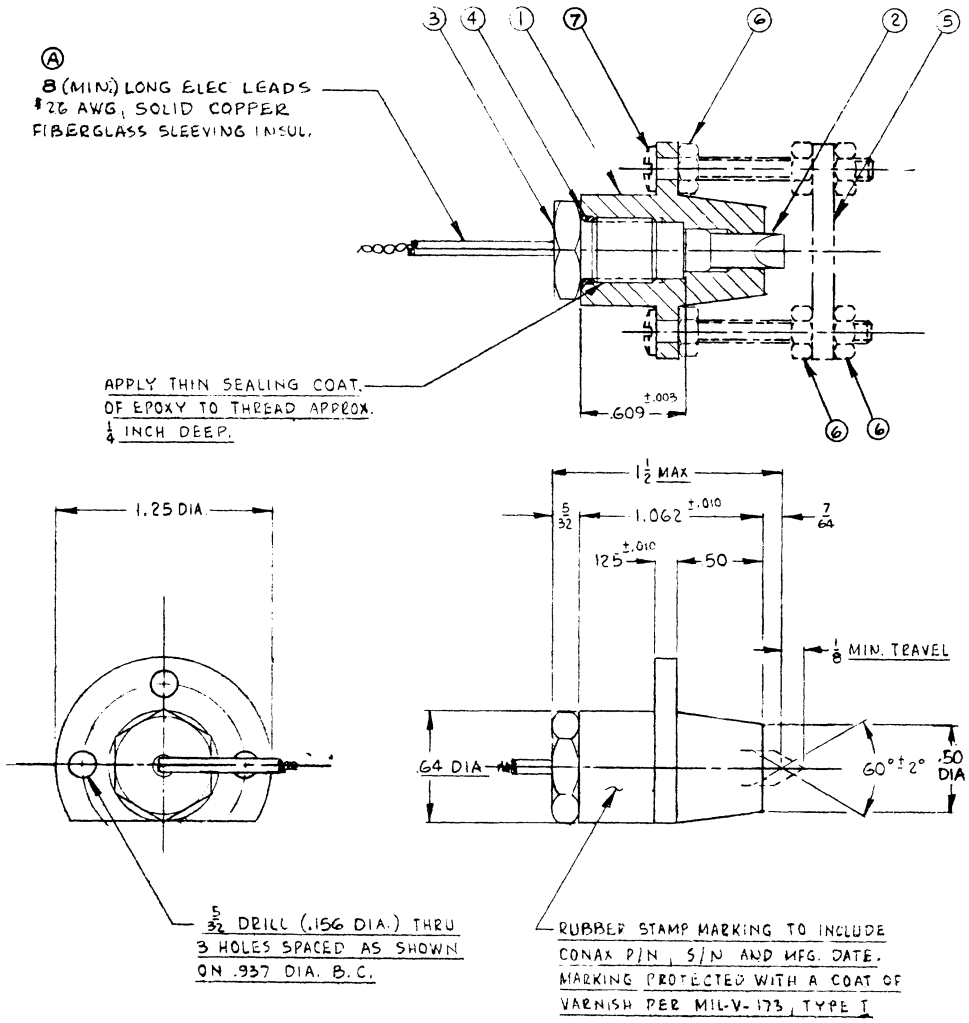

SPECIFICATIONS:-

1. ACTUATOR APPLIED FORCE	=200# MIN AT BEGINNING OF STROKE
2. PRIMER BRIDGE WIRE RESISTANCE	=0.6 - 1.2 Ω's
3. CONTINUITY TEST	=0.01 AMP
4. MAX. POSITIVE NO-FIRE	=0.15 AMP
5. MIN. POSITIVE FIRE	=1 AMP
6. RECOMM. FIRING CURRENT	=2 AMPS
7. OPERATING TIME @ 2 AMPS	=0.002 SEC.
8. OPERATING RANGE	=-60°F TO +160°F
9. ENVIRONMENTAL PRESSURE	=SEA LEVEL TO 10^{-9} ATM
10. WEIGHT EST	=1 1/2 OZ

NOTES -

1. ANODIZE ALUMINUM PARTS PER MIL-A-8625 (ASG), TYPE I

Figure 9. Conax linear actuator.

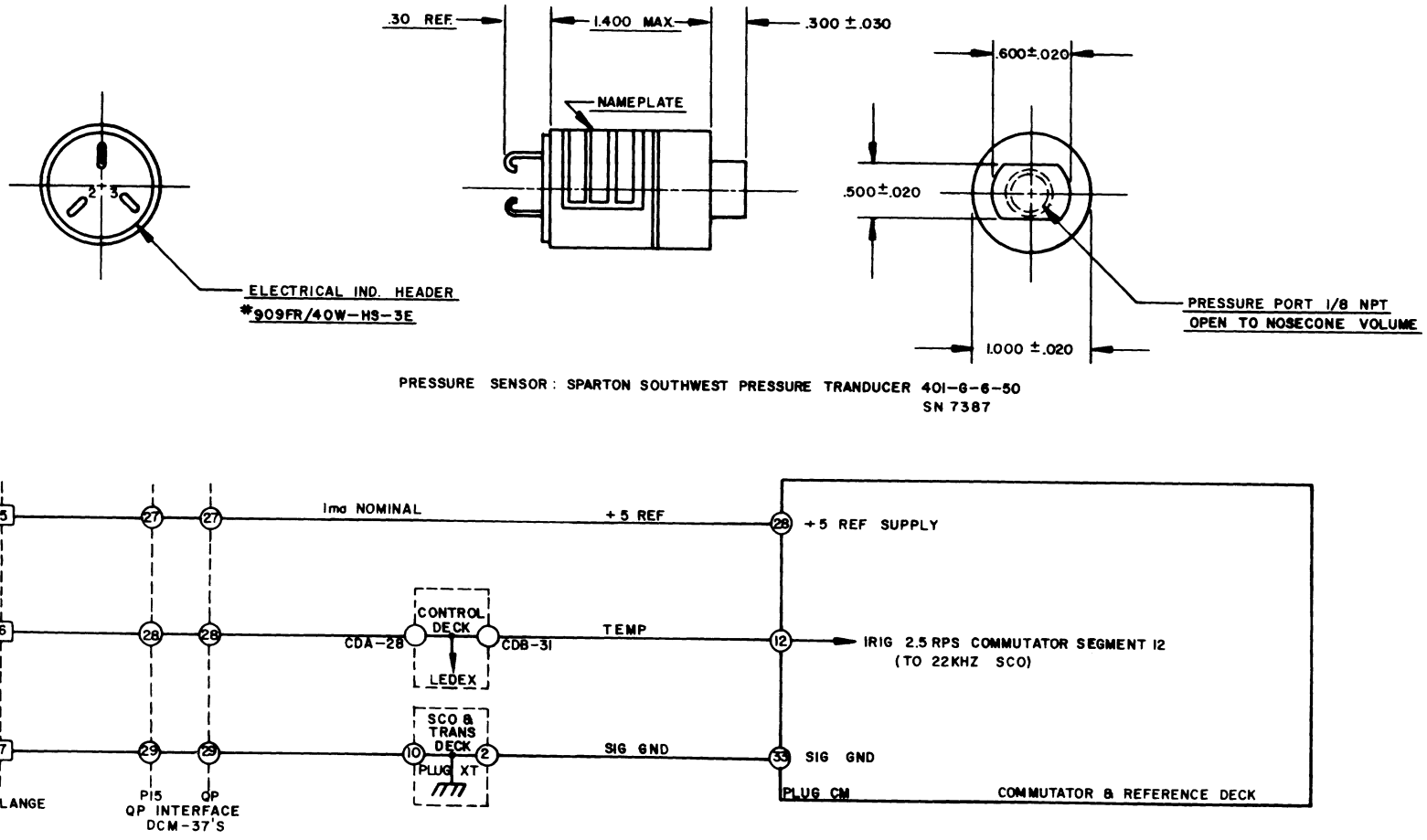

Figure 10. Pressure sensor.

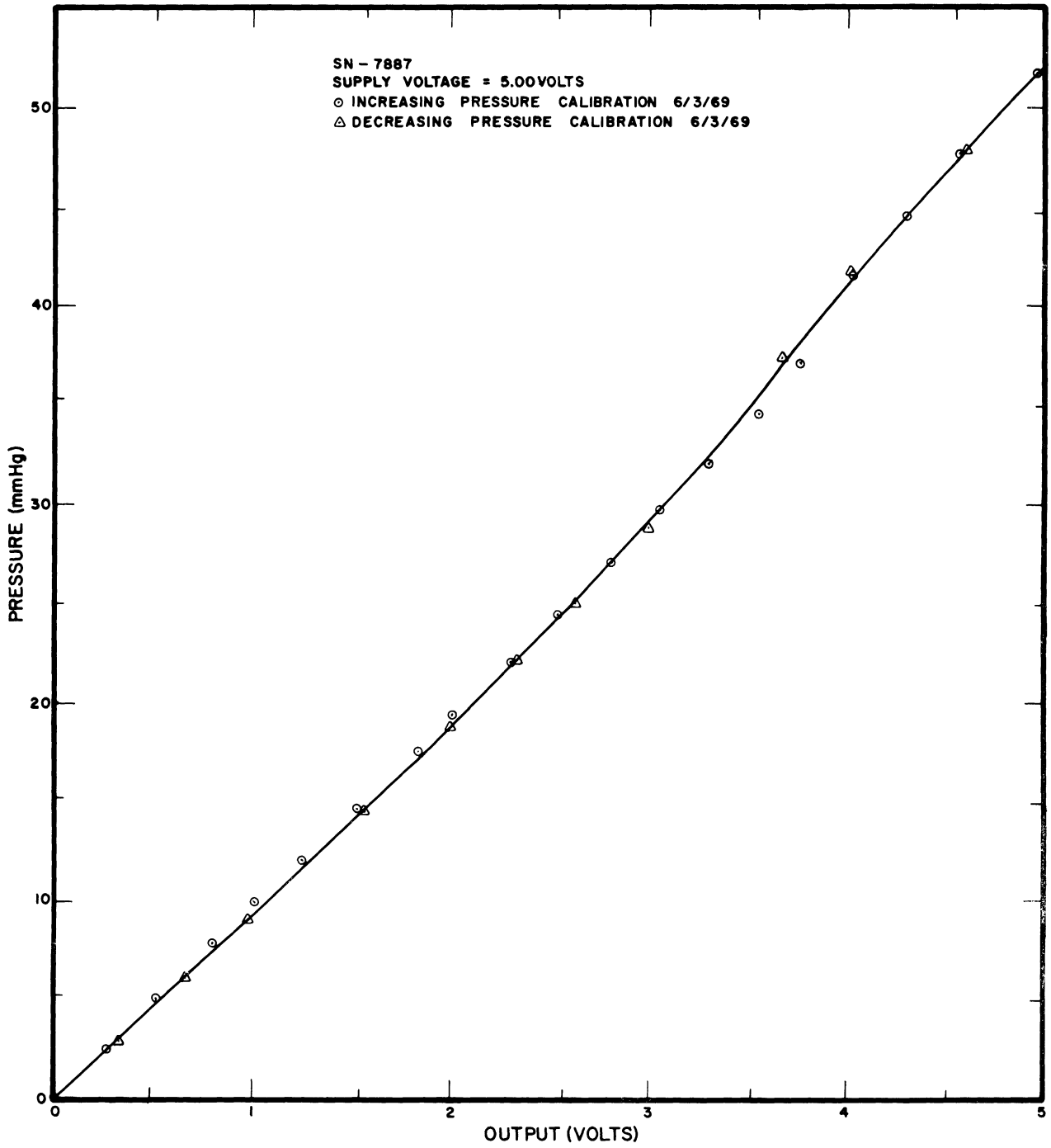

Figure 11. Pressure sensor calibration.

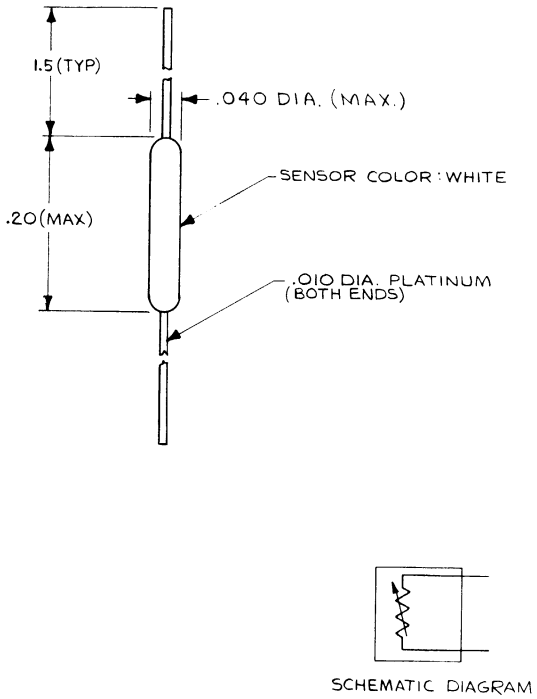

Figure 12. Temperature sensor.

ROSEMOUNT ENGINEERING COMPANY TEST REPORT

MODEL 146CY
SERIAL 3891
DATE 12 31 68
QUALITY CONTROL APPROVED

ACTUAL CALIBRATION POINTS

TEMP K	RESISTANCE
273.1500	496.89610
373.1665	690.27000

ALPHA IS .00389100
DELTA IS 1.50501
BETA IS .1100

TEMP K	RESISTANCE
300.00	549.38005
310.00	568.81997
320.00	588.20160
330.00	607.62504
340.00	626.79035
350.00	645.99742
360.00	665.14631
370.00	684.23706
380.00	703.26952
390.00	722.24384
400.00	741.15993
410.00	760.01783
420.00	778.81755
430.00	797.55900
440.00	816.24237
450.00	834.86753
460.00	853.43440
470.00	871.94313
480.00	890.39368
490.00	908.78899
500.00	927.12017
510.00	945.39810
520.00	963.61386
530.00	981.77382
540.00	999.87475
550.00	1017.91780
560.00	1035.90290
570.00	1053.82960
580.00	1071.69820
590.00	1089.50860
600.00	1107.26070
610.00	1124.95460
620.00	1142.59050
630.00	1160.16800
640.00	1177.68740
650.00	1195.14860
660.00	1212.55160
670.00	1229.89650
680.00	1247.18330
690.00	1264.41140
700.00	1281.58170
710.00	1298.69370
720.00	1315.74740
730.00	1332.74310
740.00	1349.68050
750.00	1366.55980
760.00	1383.38080
770.00	1400.14360
780.00	1416.84820
790.00	1433.49470
800.00	1450.88290
810.00	1466.61300
820.00	1483.08480
830.00	1499.49850
840.00	1515.85480
850.00	1532.15120
860.00	1548.39030
870.00	1564.57110
880.00	1580.69380
890.00	1596.75830
900.00	1612.76450
910.00	1628.71260
920.00	1644.60260
930.00	1660.43420
940.00	1676.20770
950.00	1691.92300
960.00	1707.58010
970.00	1723.17900
980.00	1738.71890
990.00	1754.20220
1000.00	1769.62660

Figure 13. Temperature sensor calibration.

4.3. TELEMETRY AND CONTROL SECTION

In the telemetry and control section, illustrated in Figure 4, the following components are contained (the number following the component is the component designation number on Figure 4): magnetometer deck (-14), temperature and filament switch deck (-13), control deck (-12), commutator deck (-11), battery deck (-10), subcarrier oscillators and transmitter deck (-9), and the thrust axis accelerometer (-1R).

The telemetry and control section provided all payload control and timing functions, battery power, telemetry signal conditioning, and the umbilical connection to the ground support console.

4.3.1. Magnetometer Deck

The main purpose of the magnetometer was to provide roll rate data. The magnetometer deck is shown in Figure 14, the interface to the payload in Figure 15, and the calibration table in Figure 16.

4.3.2. Temperature and Filament Switch Deck

Figure 17 shows the physical configuration of the electronics which perform the automatic filament switching function and the temperature sensor signal conditioning, and Figure 18 shows the temperature sensor-electronics interface.

The temperature sensor electronics, which was designed by GFSC, accepts the temperature sensor input, and then provides as input to the telemetry system a 0 to 5 V signal proportional to the sample inlet system temperature. Figure 19 is the temperature sensor circuit diagram.

The filament switch portion of this deck provides two functions. First, it allows selection of either filament in the spectrometer ion source through the ground support console; and second, in case of a filament A (preferred) failure during flight, filament B is automatically switched in. Filament A functioned throughout this flight and a switch to filament B was not required. The filament switching circuitry is shown in Figure 20.

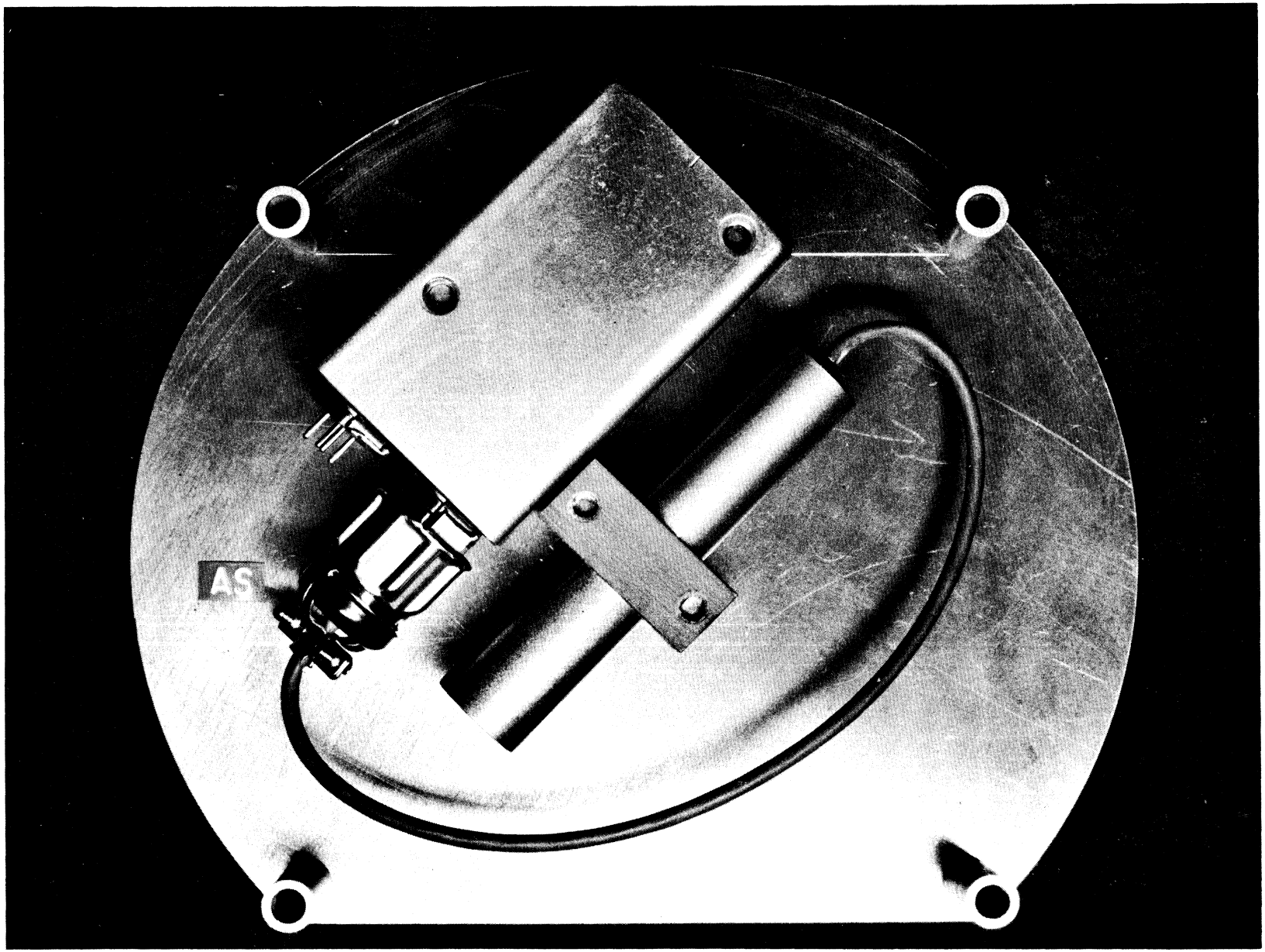

Figure 14. Magnetometer deck.

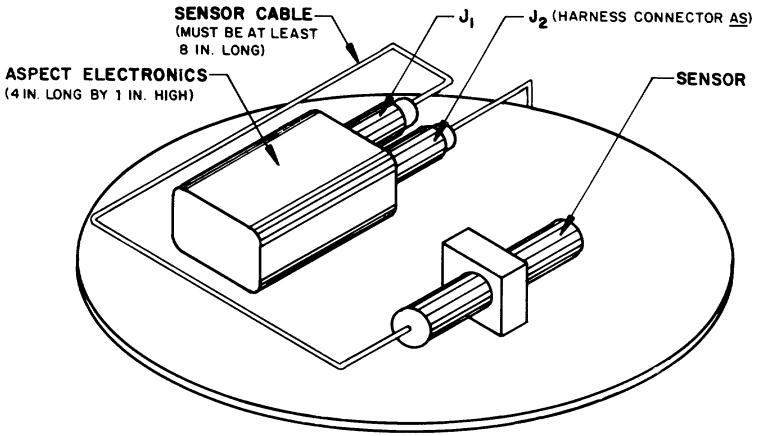

MECH. DWG. C-024-025

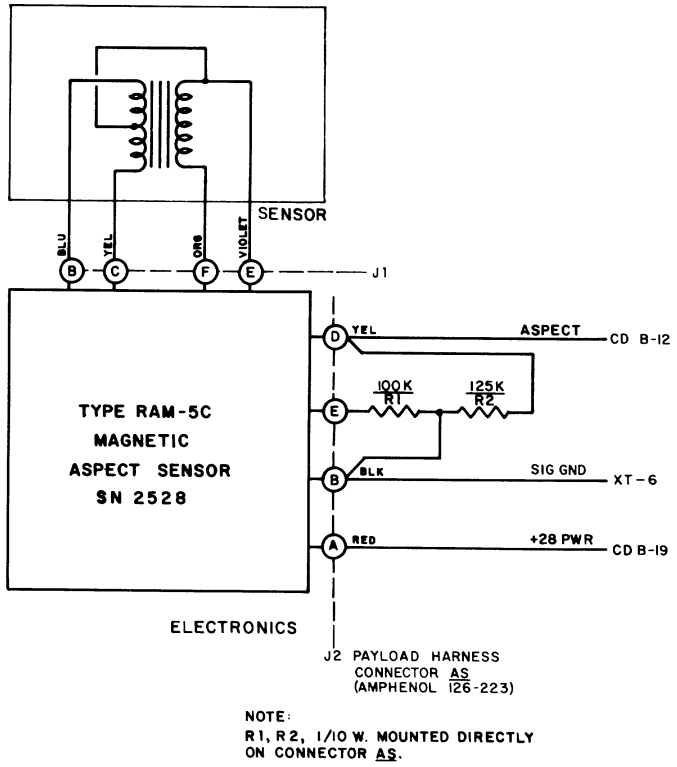

NOTE:
R1, R2, 1/10 W. MOUNTED DIRECTLY
ON CONNECTOR AS.

Figure 15. Magnetometer deck interface.

HELIFLUX®
MAGNETIC ASPECT SENSOR
TYPE RAM-5C

SERIAL NO 2528

CALIBRATION DATA

FIELD IN MILLIGAUSS	OUTPUT SIGNAL IN VOLTS D C	
600	4.78	
550	4.59	
500	4.39	
450	4.19	
400	4.00	
350	3.80	
300	3.60	
250	3.40	
200	3.20	
150	3.00	
100	2.80	
50	2.60	
0	2.40	(BIAS LEVEL)
-50	2.20	
-100	2.00	
-150	1.80	
-200	1.60	
-250	1.40	
-300	1.20	
-350	0.99	
-400	0.79	
-450	0.59	
-500	0.39	
-550	+0.19	
-600	0.00	

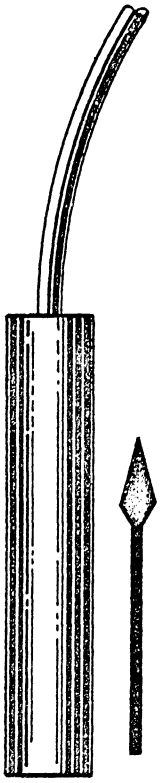

DIRECTION OF MAGNETIC FIELD FOR VOLTAGE SIGNALS ABOVE BIAS LEVEL

NOTE:
CALIBRATION MADE WITH A 100K OHM RESISTOR FROM SIGNAL OUTPUT TO NEGATIVE TERMINAL OF BATTERY SOURCE, AND A 100K OHM RESISTOR FROM BIAS OUTPUT TO NEGATIVE TERMINAL OF BATTERY SOURCE

SCHONSTEDT INSTRUMENT COMPANY
SILVER SPRING, MARYLAND

CALIBRATED BY Jimmy Brown

CALIBRATION MADE WITH BATTERY SUPPLY OF 28.8 VOLTS DATE 7-25-68

11262

Figure 16. Magnetometer calibration.

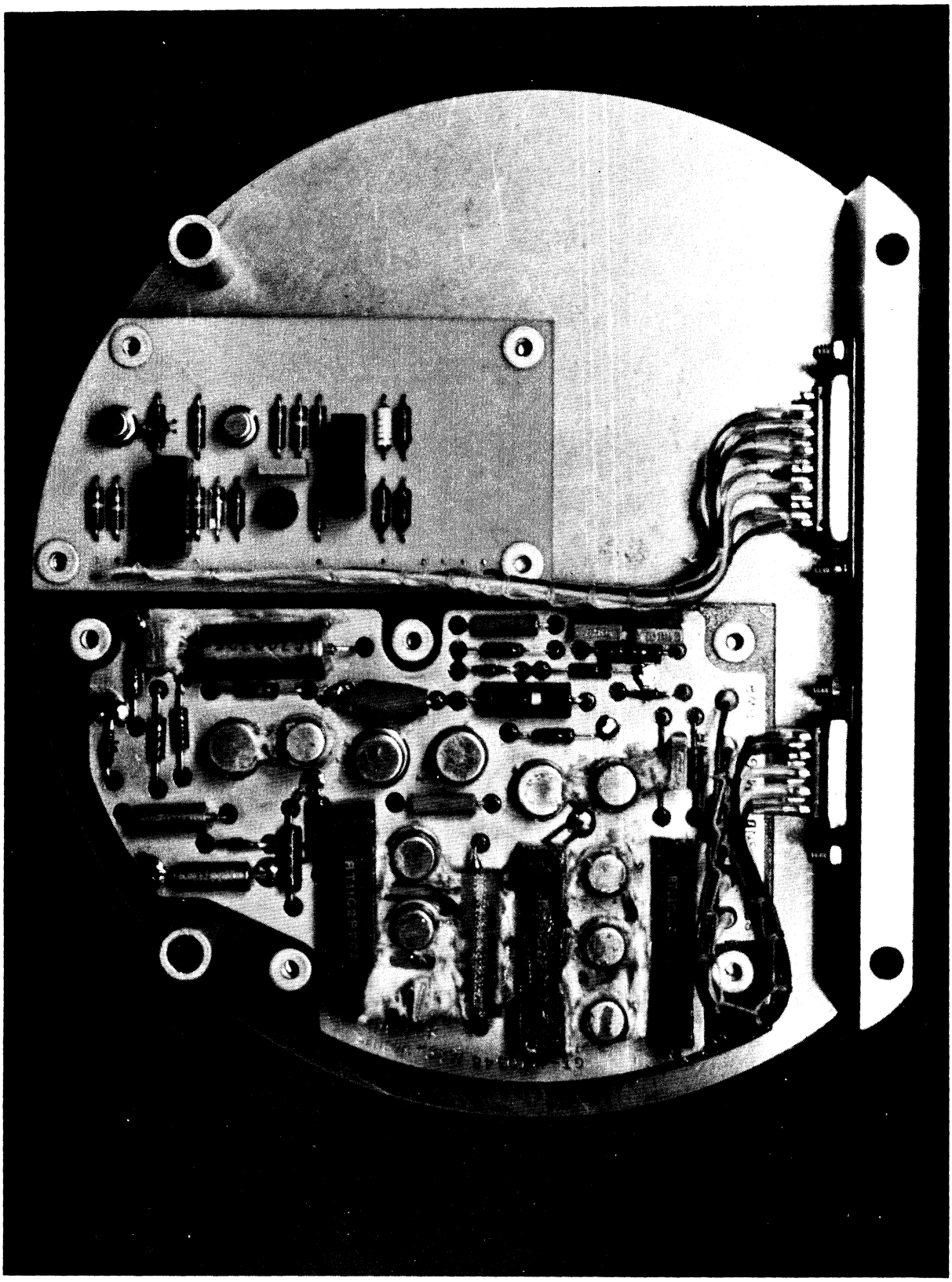

Figure 17. Temperature sensor and filament switch deck.

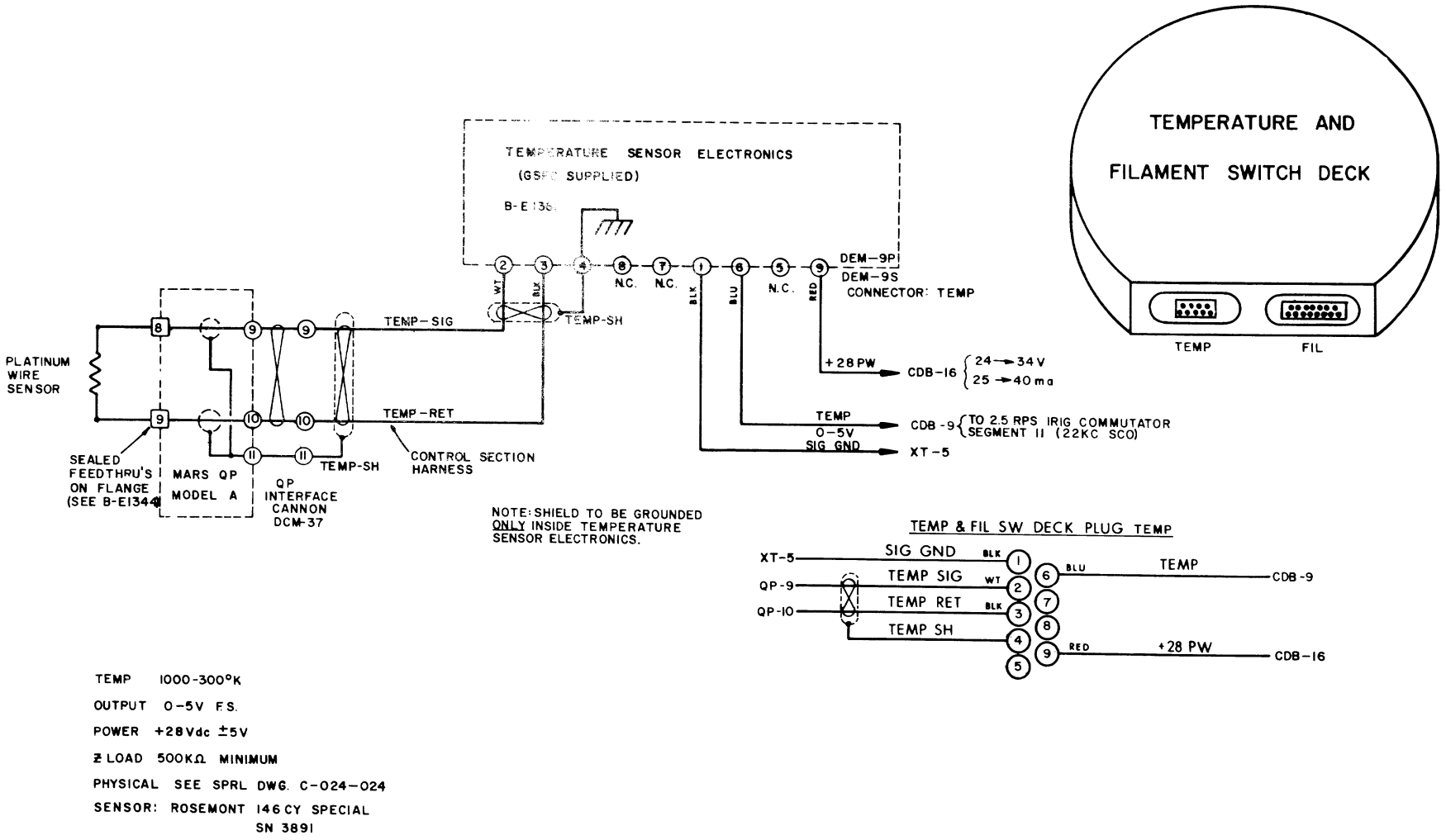

Figure 18. Temperature sensor deck interface.

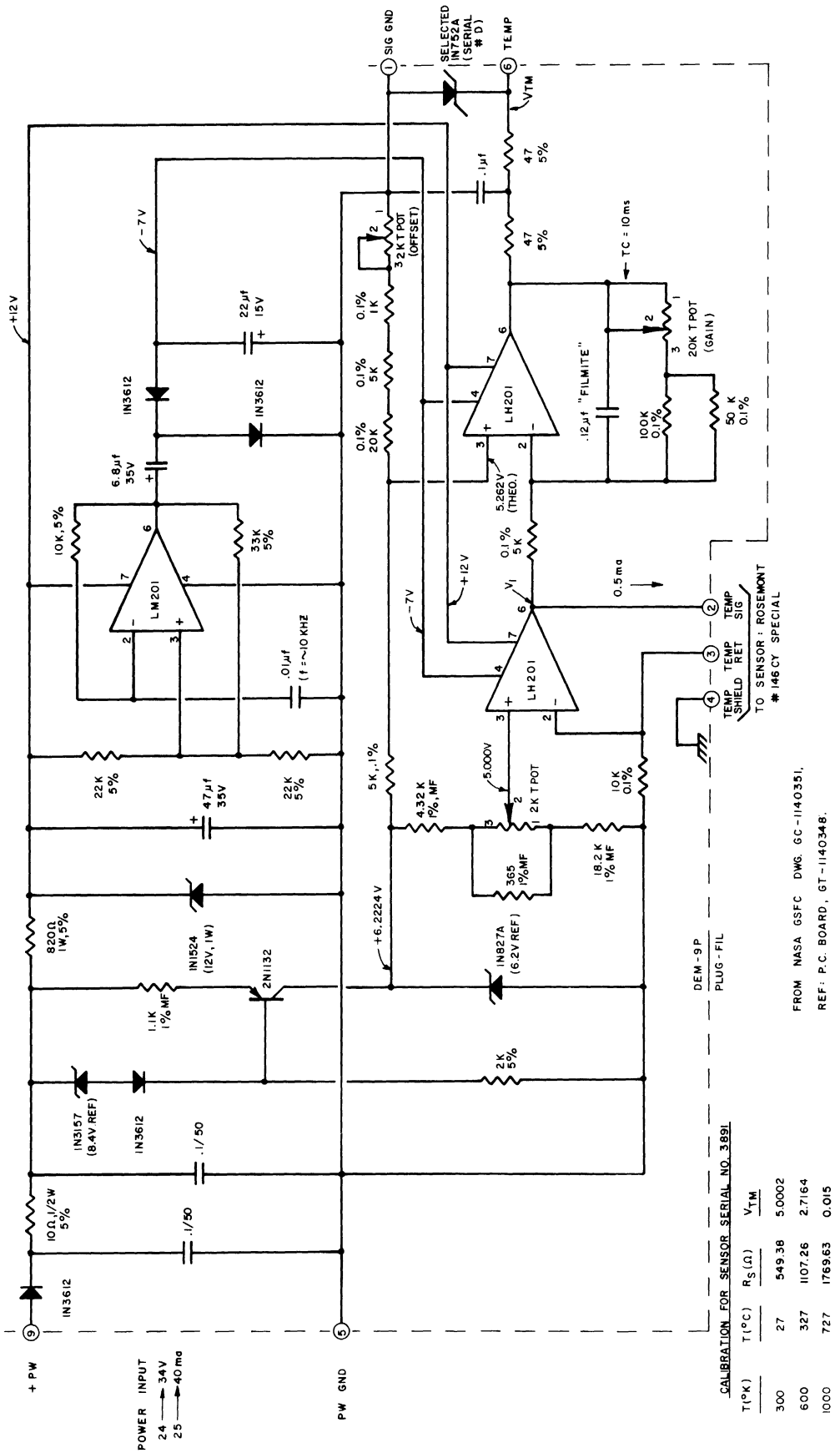

Figure 19. Temperature sensor electronics.

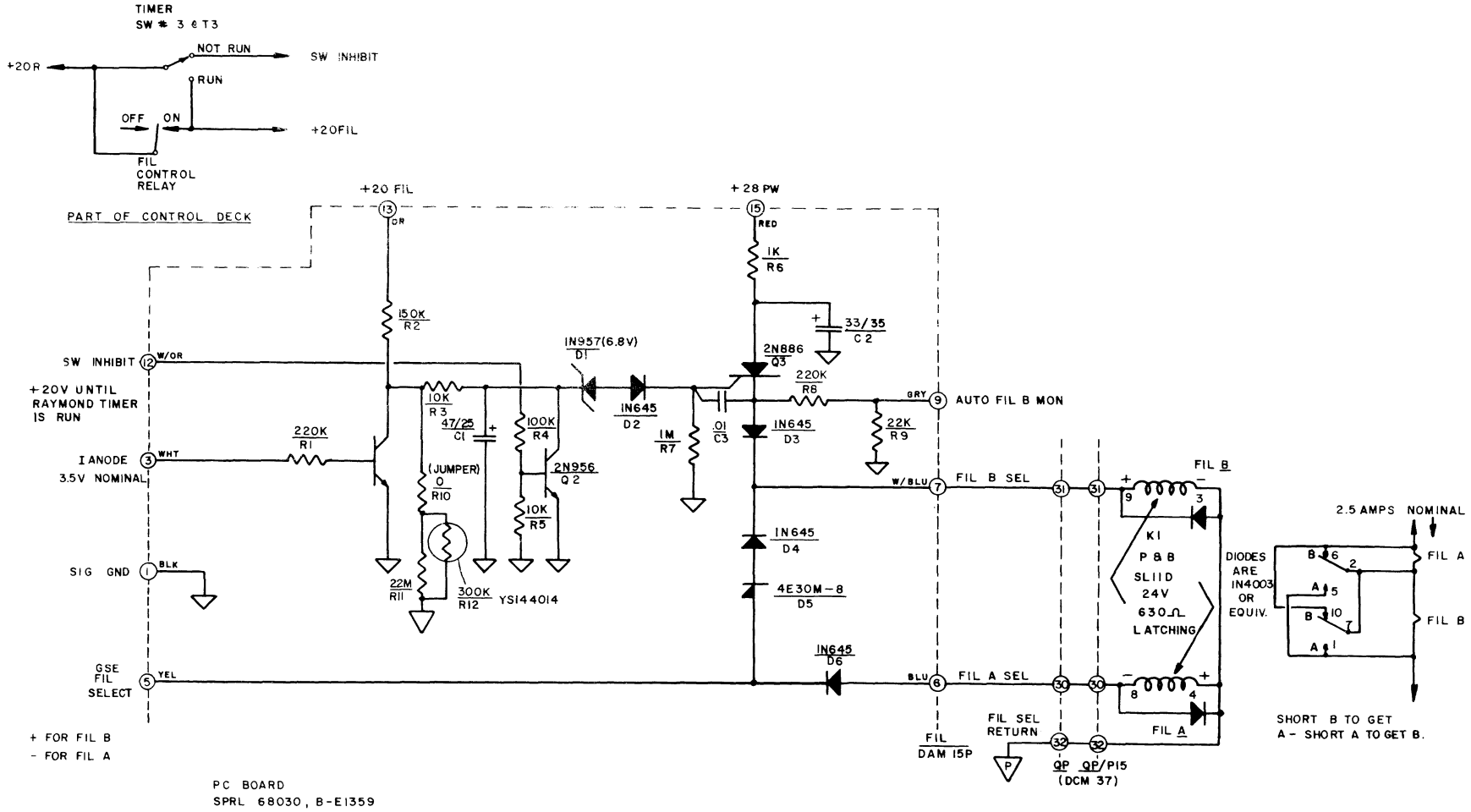

Figure 20. Automatic filament switching circuit.

4.3.3. Control Deck

The control deck is shown in Figure 21 and the payload/control deck interface is shown in Figure 22. Figures 23 and 24 show the circuitry involved in the control deck. The control deck contains the Raymond "G" timer, the Ledex rotary stepping switch, the internal/external power control, and the mass spectrometer ion source filament on/off control.

The Raymond "G" timer was actuated at lift-off and provided three timing signals: at T+15 sec backup power was supplied to the entire payload; at T+19 sec redundant filament power was supplied and, after a three sec delay to allow for filament stabilization, the automatic filament switching circuit was enabled; and at T+24.5 sec the pyrotechnic activating signal was generated, thus opening the mass spectrometer breakoff device.

The Ledex rotary switch provided power to various payload components and supplied various monitor points to the ground support control console depending on which of twelve possible positions it was in. The table of functions and monitors is shown in Figure 25.

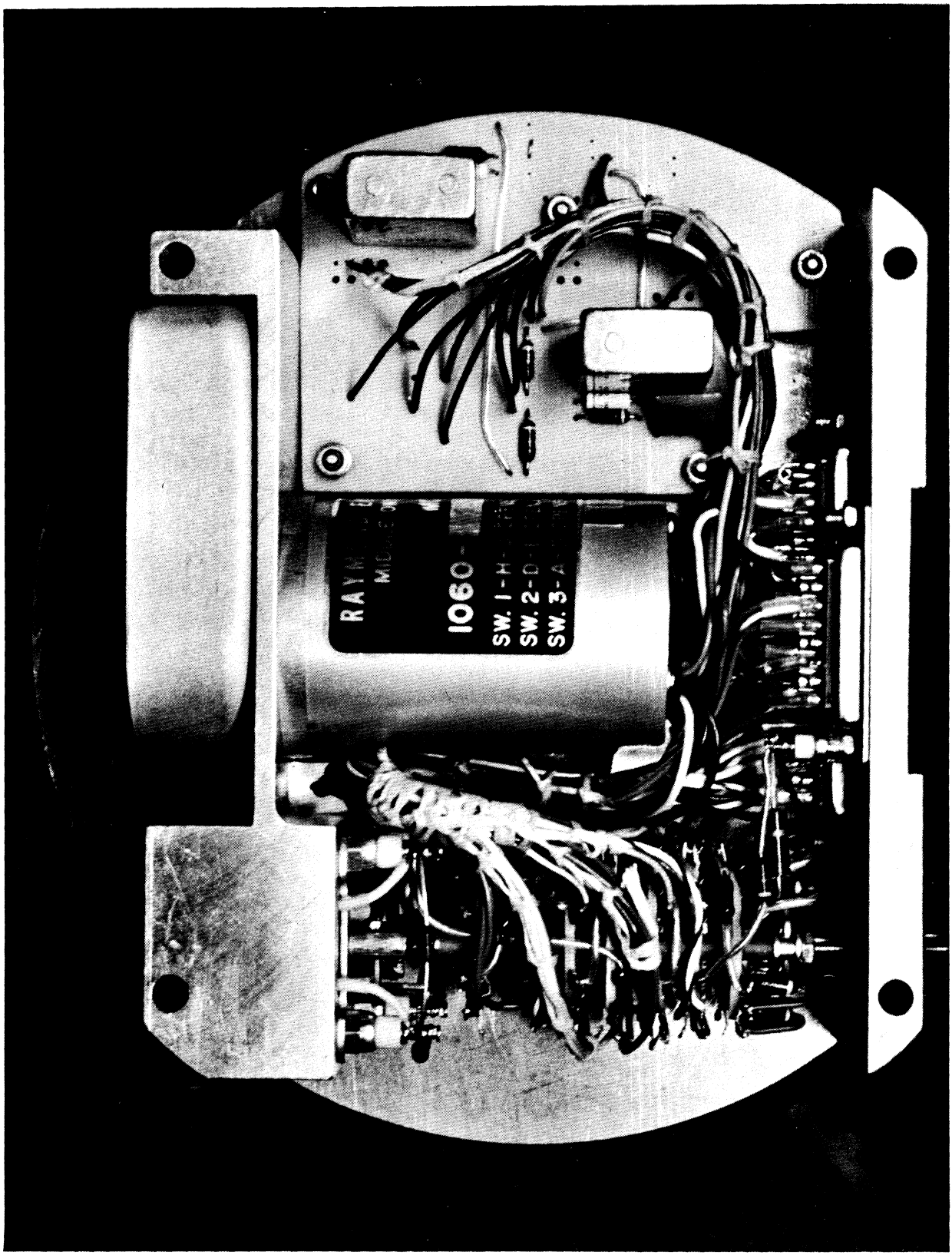

Figure 21. Control deck.

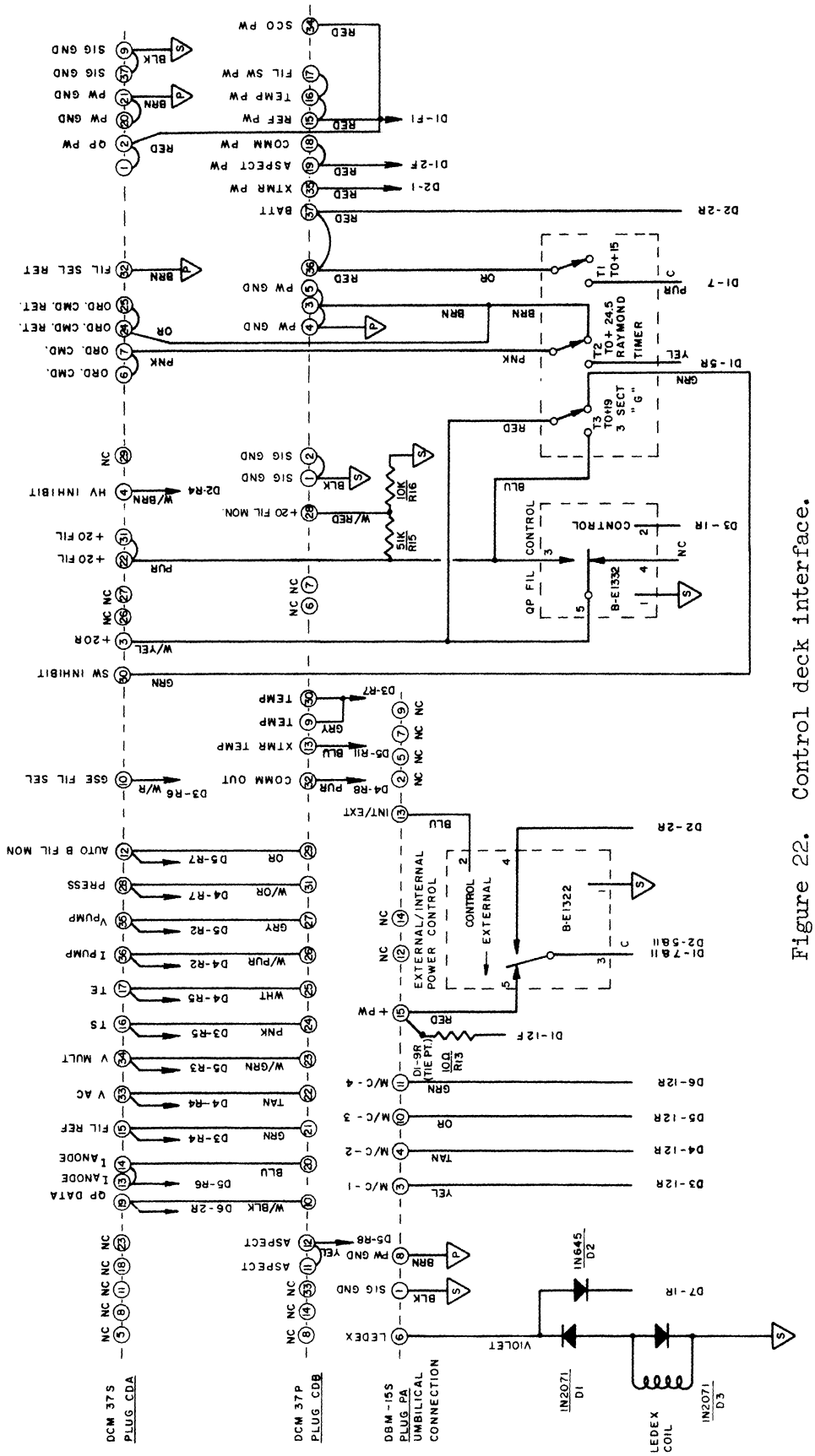

Figure 22. Control deck interface.

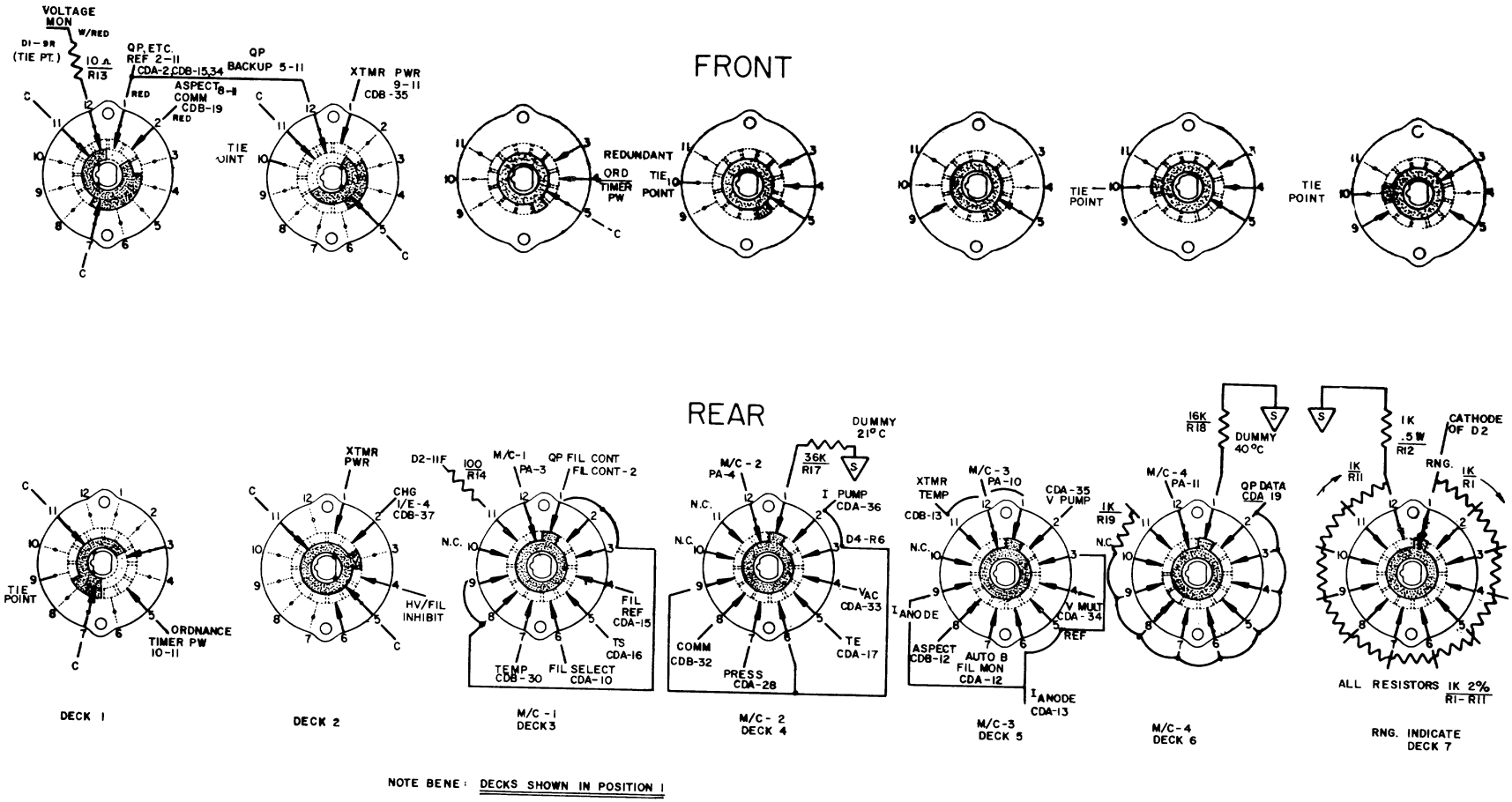

Figure 23. Control deck index wiring.

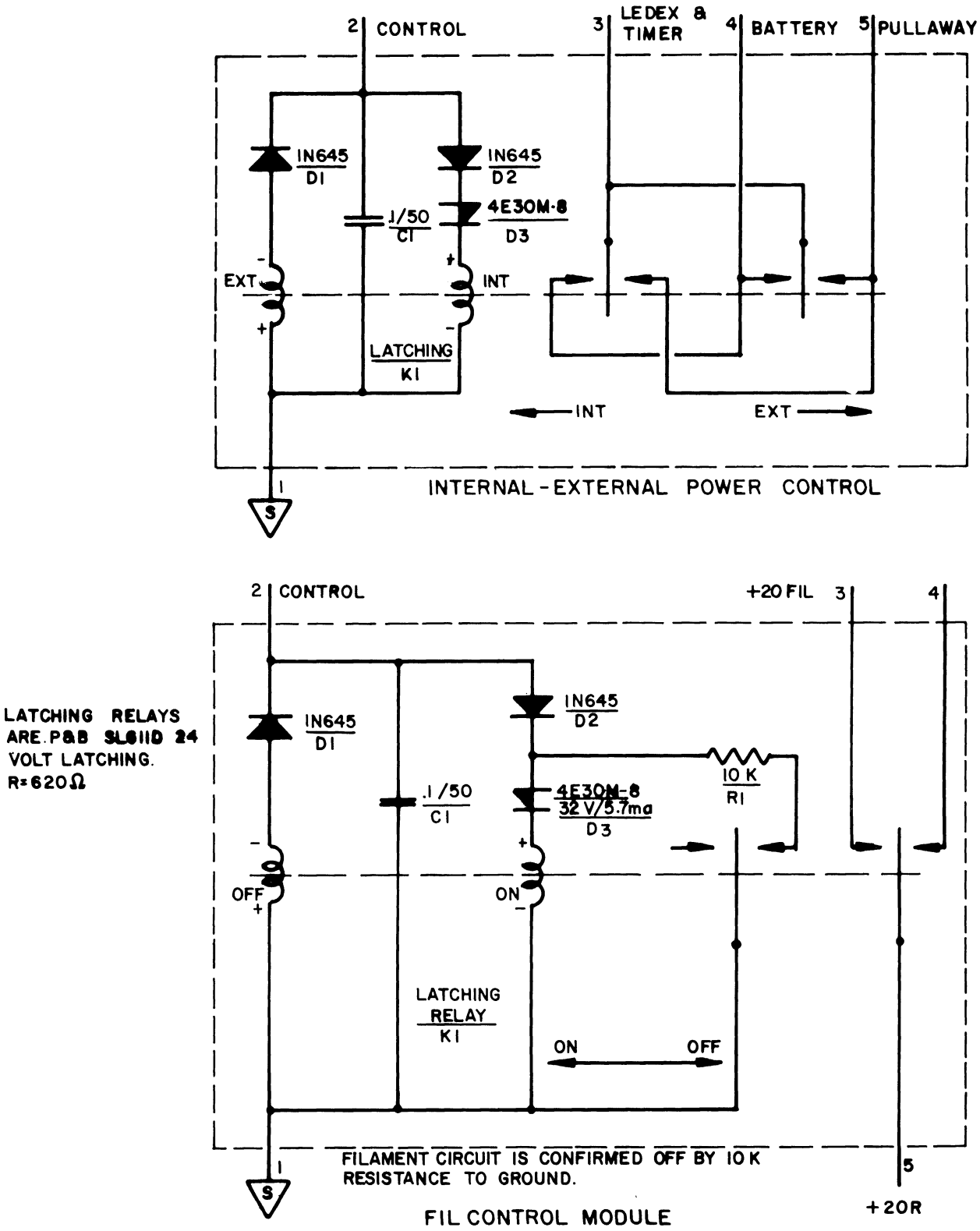

Figure 24. Control deck circuits.

LEDEX POSITION	POWER									FUNCTIONS	MONITOR / CONTROL LEADS			
	VOLTAGE MONITOR R=10Ω	QP, SCO REF, CAL TEMP, PRESS	ASPECT COMM	XTMR	TIMER COMMON	QP HV INHIBIT					1	2	3	4
1	X									UMBILICAL CONTINUITY	QP FIL CONTROL	DUMMY THERM 21°C	XTMR TEMP	DUMMY THERM 40°C
2		X				X				QP CHECK	QP FIL CONTROL	I PUMP	V PUMP	QP DATA
3										" "	QP FIL CONTROL	I PUMP	I_{ANODE}	QP DATA
4										" "	FIL REF	V_{AC}	V MULT	QP DATA
5										" "	T_s	TE	I ANODE	QP DATA
6										" "	FIL SELECT	I PUMP	I ANODE	QP DATA
7										TEMP & PRESS	TEMP	PRESSURE	AUTO B FIL MON	QP DATA
8			X							COMMUTATOR & ASPECT	QP FIL CONTROL	COMMUTATOR	ASPECT	QP DATA
9				X						XTMR ON	QPFIL CONTROL	I PUMP	I ANODE	QP DATA
10										PREFLIGHT CHECK	OPEN	OPEN	OPEN	OPEN
11										FLIGHT	BAT MON R=100Ω	OPEN	XTMR TEMP	QP DATA R=1K
12					X CHARGE					BATTERY CHARGE	OPEN	OPEN	OPEN	OPEN

NOTE: I/E CONTROL ACTIVE IN ALL POSITIONS.

Figure 25. Control functions and monitors.

4.3.4. Commutator Deck

The commutator deck, shown in Figure 26, contains the commutator and the 0 through 5 V precision reference supply voltages. The circuit and the interface diagrams are shown in Figure 27 and the commutator is shown in Figure 28.

The commutator cyclically sampled its 30 inputs at the rate of 75 samples per second and supplied these sampled data to the telemetry system. The commutator segment assignments were as follows:

Segment No.	Segment Assignment	
1	mass spectrometer anode current	I_a
2	mass spectrometer filament reference	fil ref
3	mass spectrometer quadrupole rod voltage	V_{ac}
4	mass spectrometer multiplier voltage	V_{mult}
5	mass spectrometer ion source temperature	T_s
6	mass spectrometer electronics temperature	T_E
7	mass spectrometer vac ion pump current	I_p
8	mass spectrometer vac ion pump voltage	V_p
9	mass spectrometer +20 V filament monitor	0 V = fil off
10	mass spectrometer automatic B filament	0 V = fil A
11	temperature	
12	pressure	
13	battery voltage/6	
14	transmitter temperature	
15	zero reference	
16	mass spectrometer anode current	I_a
17	mass spectrometer filament reference	fil ref
18	mass spectrometer quadrupole rod voltage	V_{ac}
19	mass spectrometer multiplier voltage	V_{mult}
20	mass spectrometer ion source temperature	T_s
21	mass spectrometer electronics temperature	T_E
22	mass spectrometer vac ion pump current	I_p
23	mass spectrometer vac ion pump voltage	V_p
24	0 V reference	
25	1 V reference	
26	2 V reference	
27	3 V reference	
28	4 V reference	
29	5 V reference and frame sync	
30	5 V reference and frame sync	

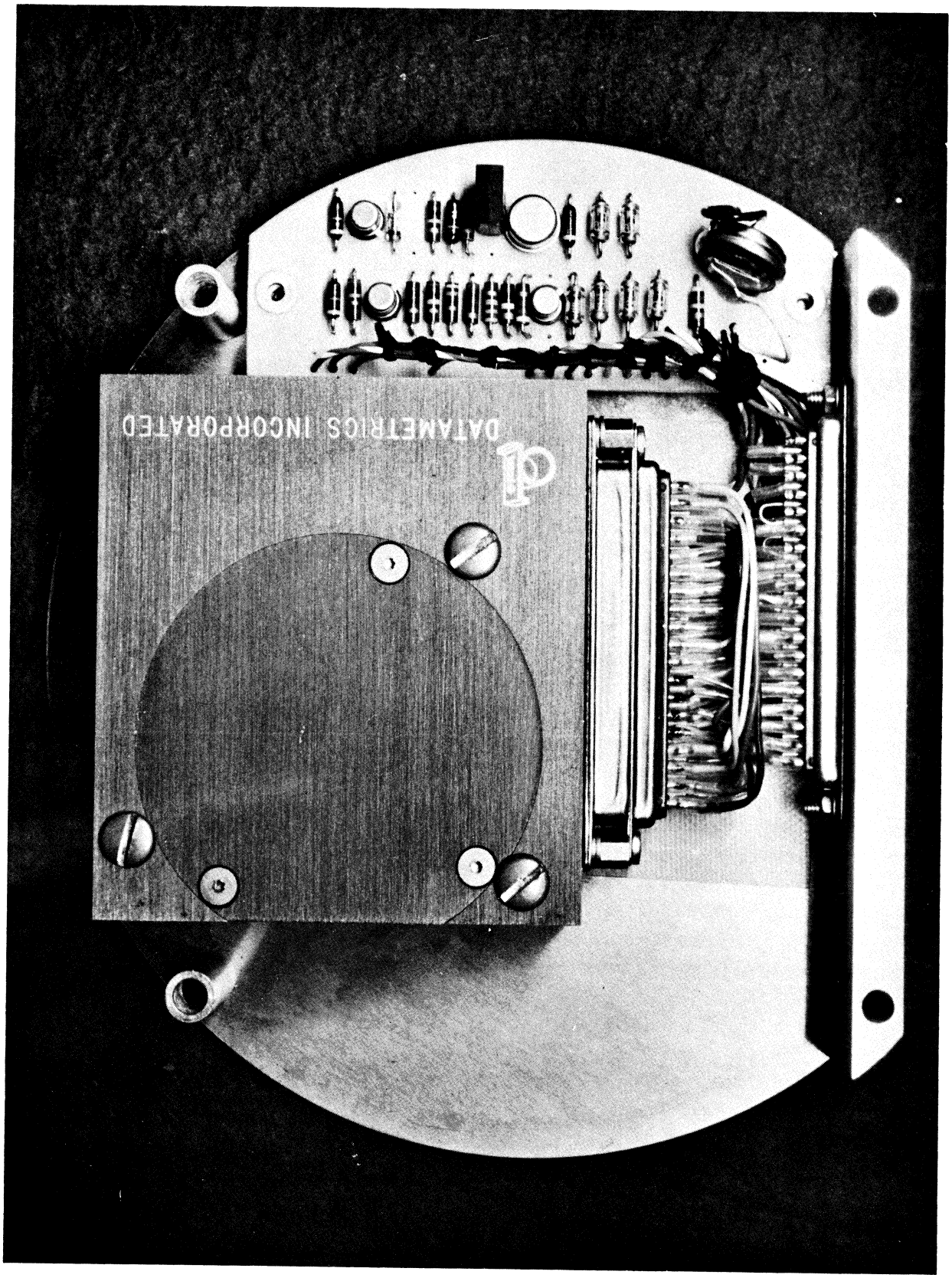

Figure 26. Commutator deck.

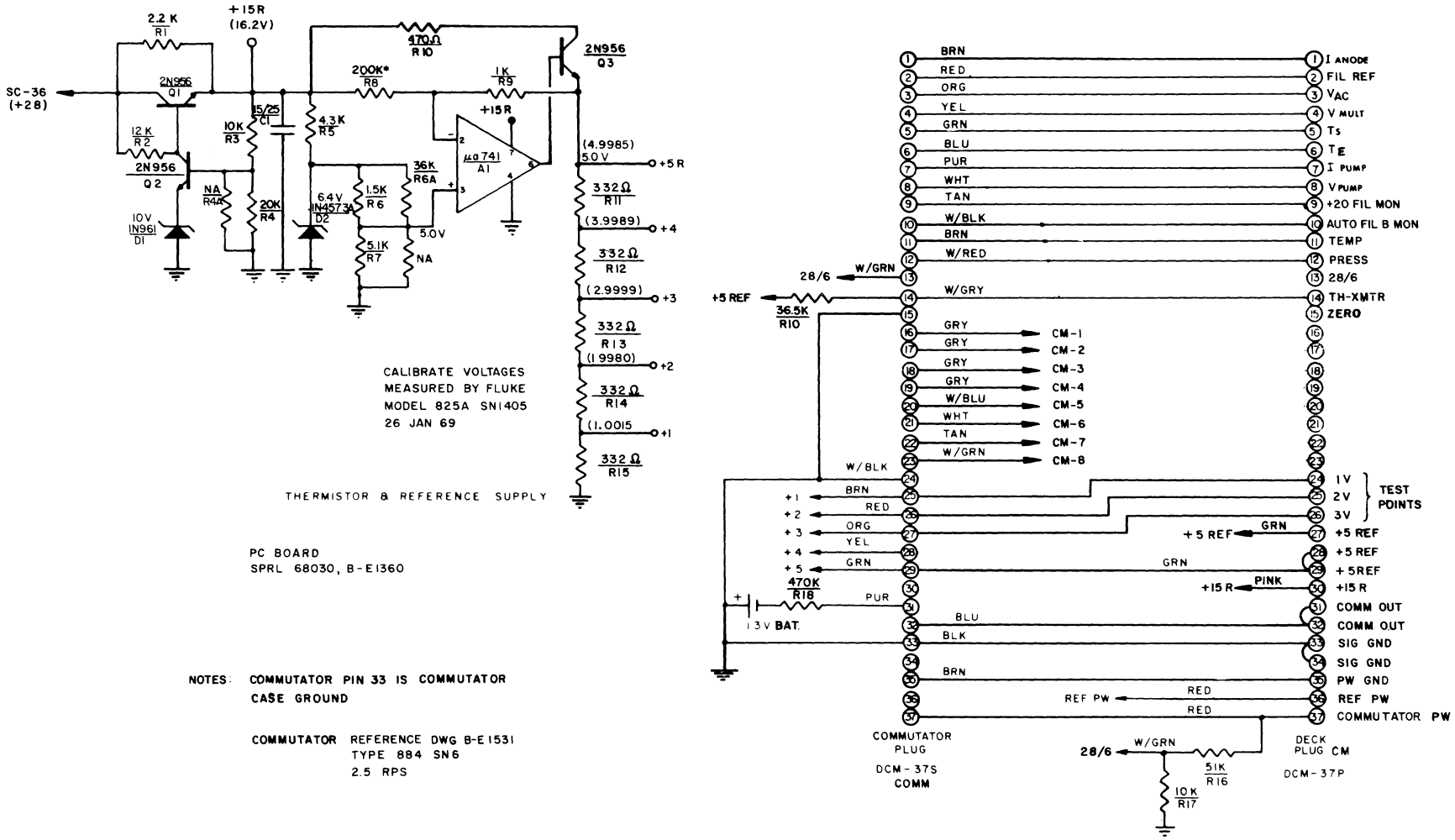

Figure 27. Commutator deck interface and reference supply circuit.

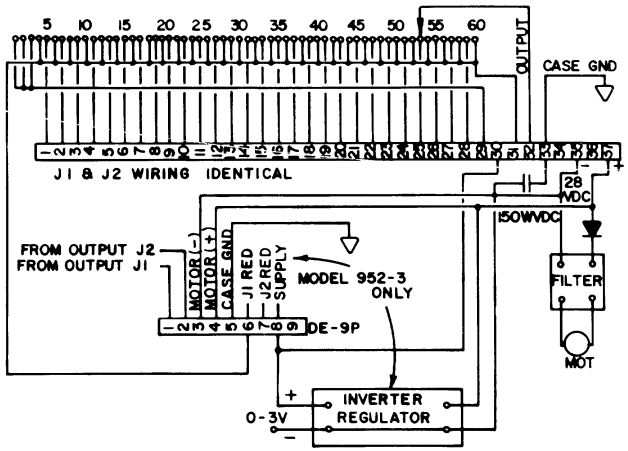

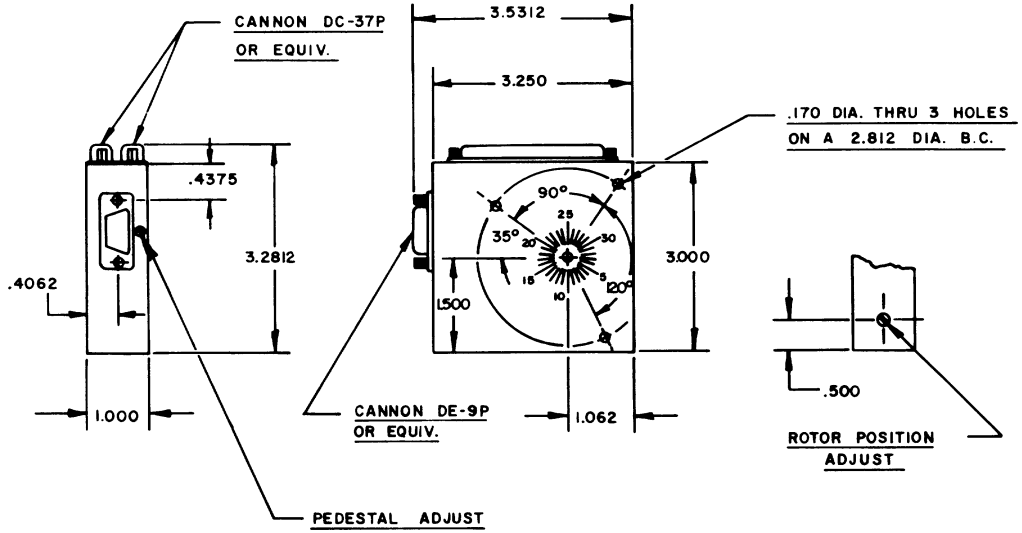

NOTES:
1. TWO POLES.
2. FRAME RATE: (AT 28 ±3% VOLTS) SEE TABULATION BLOCK.
3. PHASING: NOMINAL COINCIDENT "ON" TIME OF CORRESPONDING DATA POINTS.
4. MOTOR VOLTAGE: 28 VOLTS AT 2 WATTS MAX.
5. CONTACT RATING: 50 VOLTS, 50 MA, MAX.
6. CONTACT RESISTANCE: LESS THAN 1Ω.
7. NOISE: LESS THAN 20 μVOLTS, RMS, 0-10 KC BANDWIDTH DURING CONTACT "ON" TIME.
8. LEAKAGE RESISTANCE: GREATER THAN 100 MEGOHMS AT 250 VOLTS, MAX.
9. WEIGHT: 11.02 MAX.
10. ENVIRONMENTAL:
    A. SHOCK: 150 G'S, 11 MILLISEC, ANY AXIS.
    B. VIBRATION: 35 G'S, 20 TO 2000 CPS, ANY AXIS.
    C. 125 G'S, ANY AXIS.
    D. OPERATING TEMP. RANGE: -55°F TO +175°F.
    E. ALTITUDE: UNLIMITED, 10 HRS MAX EXPOSURE TO HARD VACUUM.
11. SWITCH FORMAT (BOTH POLES) FOR AUTOMATIC DECOMMUTATION.
    A. 28 DATA POINTS - DUTY CYCLE 52% ±5% OF CHANNEL INTERVAL.
    B. FRAME SYNC SEG: 150% ± 5% OF CHANNEL INTERVAL.
    C. COLLECTOR ACTION: BBM.
    D. PEDESTAL VOLT: 0 - +3V (REL TO MINUS SIDE OF PWR LINE).
    E. STABILITY: 1% OF SETTING UNDER ALL OPERATING CONDITIONS.

TYPE NO.	FRAME RATE
TYPE 952-3 *	2.5 RPS, +5, -15%
TYPE 953-3	5 RPS, +5, -15%
TYPE 951-2	1 RPS, +5, -15%

* (884) 37 PIN CONNECTOR USES SAME WIRING AS (952-3).

Figure 28. Commutator.

4.3.5. Battery Deck

The battery deck is shown in Figure 29 and the schematic and payload interface is shown in Figure 30. The battery deck supplies internal power for the entire payload including the Conax linear actuators.

4.3.6. Subcarrier Oscillator and Transmitter Deck

The SCO and transmitter deck, shown in Figure 31, contains the transmitter, mixer amplifier, four subcarrier oscillators (SCO's), and the SCO calibration systems. The components for this PAM/FM/FM telemetry system were supplied by the Sounding Rocket Branch of Goddard Space Flight Center and the telemetry system was then assembled, calibrated, and tested by the Space Physics Research Laboratory. The interconnection diagram for this deck is shown in Figure 32.

The SCO calibration system was designed to place 0 and 5 V, 50 msec pulses on each of three SCO channels every 15 sec. The commutator SCO was not calibrated in this manner since a six-point calibration was included in commutator segments 24 through 30. The SCO calibration block diagram is shown in Figure 33 and the component circuitry is shown in Figure 34.

4.3.7. Thrust Axis Accelerometer

The thrust axis accelerometer, Figure 35, was provided by the Sounding Rocket Branch of Goddard Space Flight Center to monitor the performance of the rocket motors. The accelerometer operated satisfactorily throughout the flight.

4.4. PYROTECHNIC FIRING CIRCUITS

The pyrotechnic firing circuits are shown in Figure 36. As can be seen, battery power is connected to the Raymond timer only in Ledex positions 10 (pre-flight check) and 11 (flight). After lift-off but before the mass spectrometer inlet opening, the Raymond timer kept a direct short across both Conax linear actuators to protect against premature firing due to transient or spurious radiated signals. At T+24.5 sec the timer removed the short and applied full battery voltage across the redundant Conax linear actuators. Four current limiting resistors were placed in series with the actuators to protect the battery in case an actuator should present a short after firing. In addition, the timer contact was only a momentary closure. The pyrotechnic firing circuit and breakoff device performed as required for this shot.

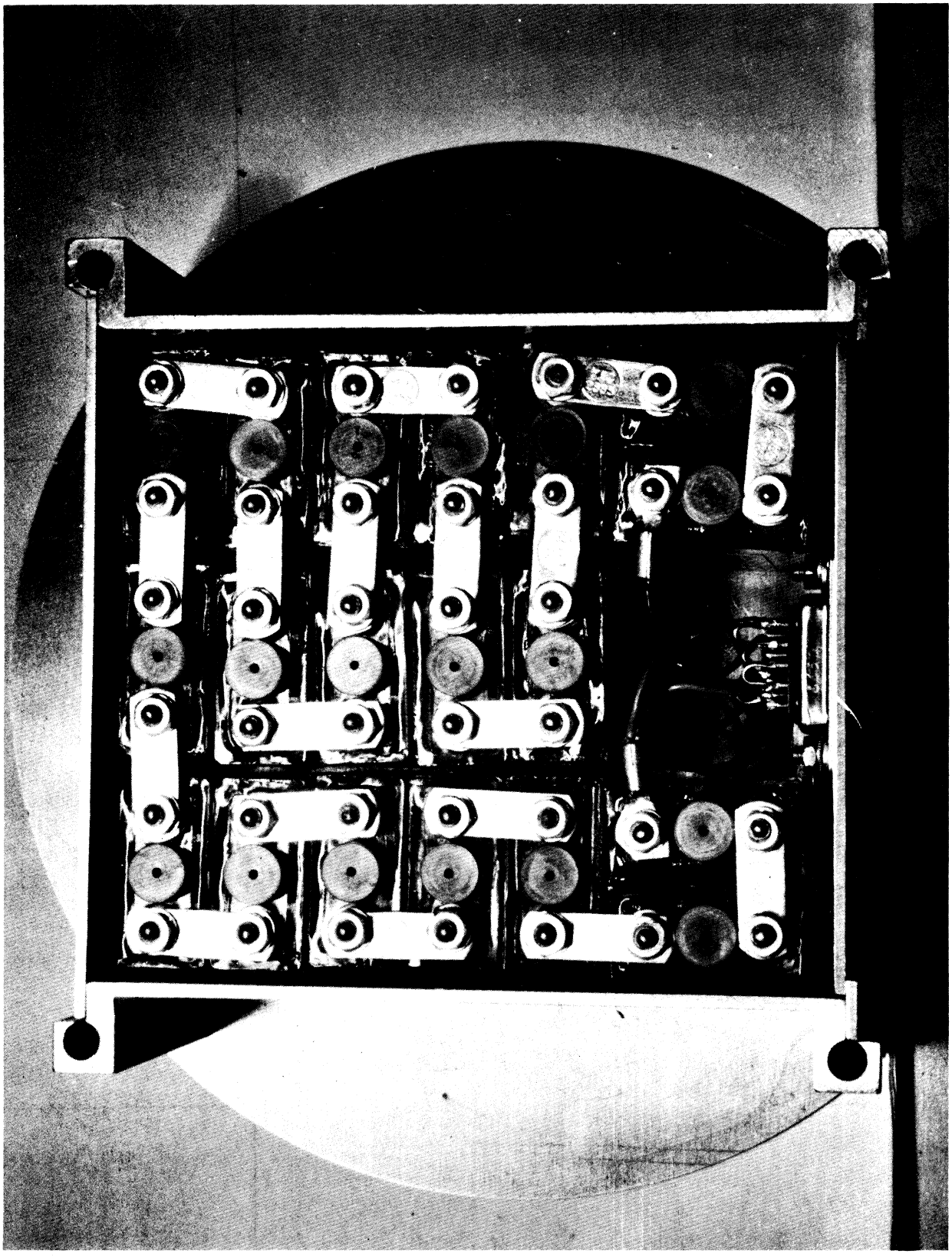

Figure 29. Battery deck.

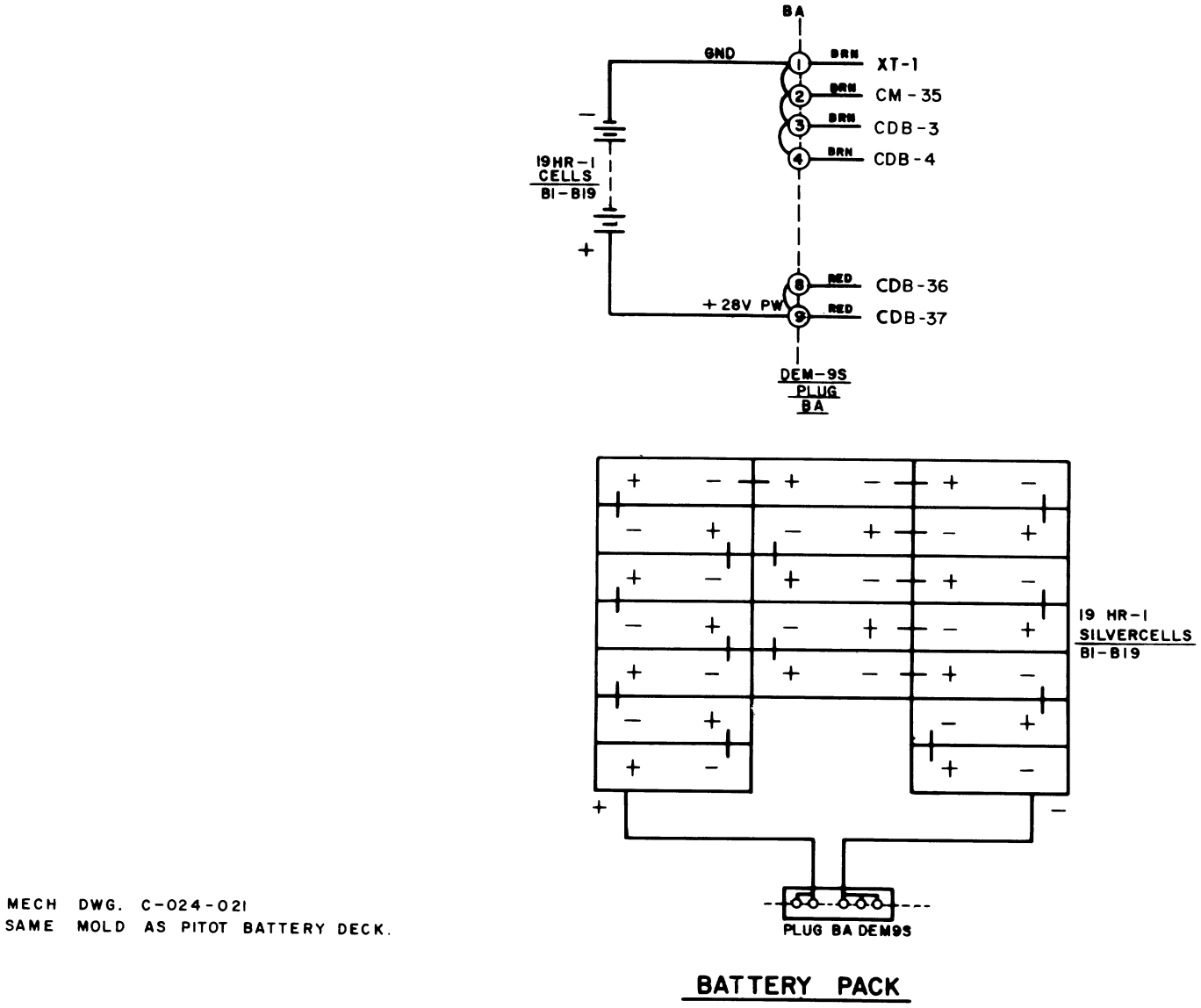

Figure 30. Battery deck interface.

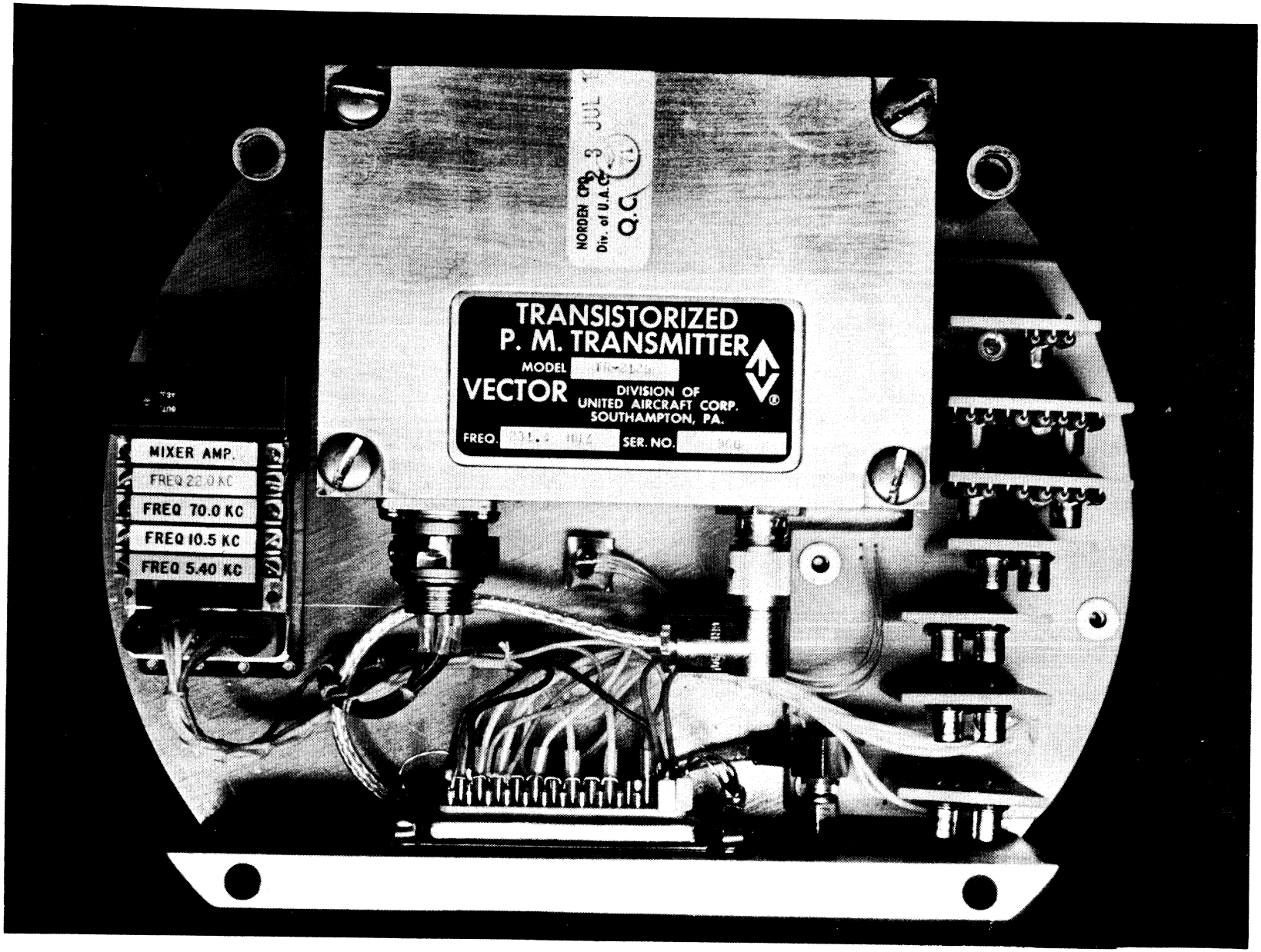

Figure 31. Subcarrier oscillator and transmitter deck.

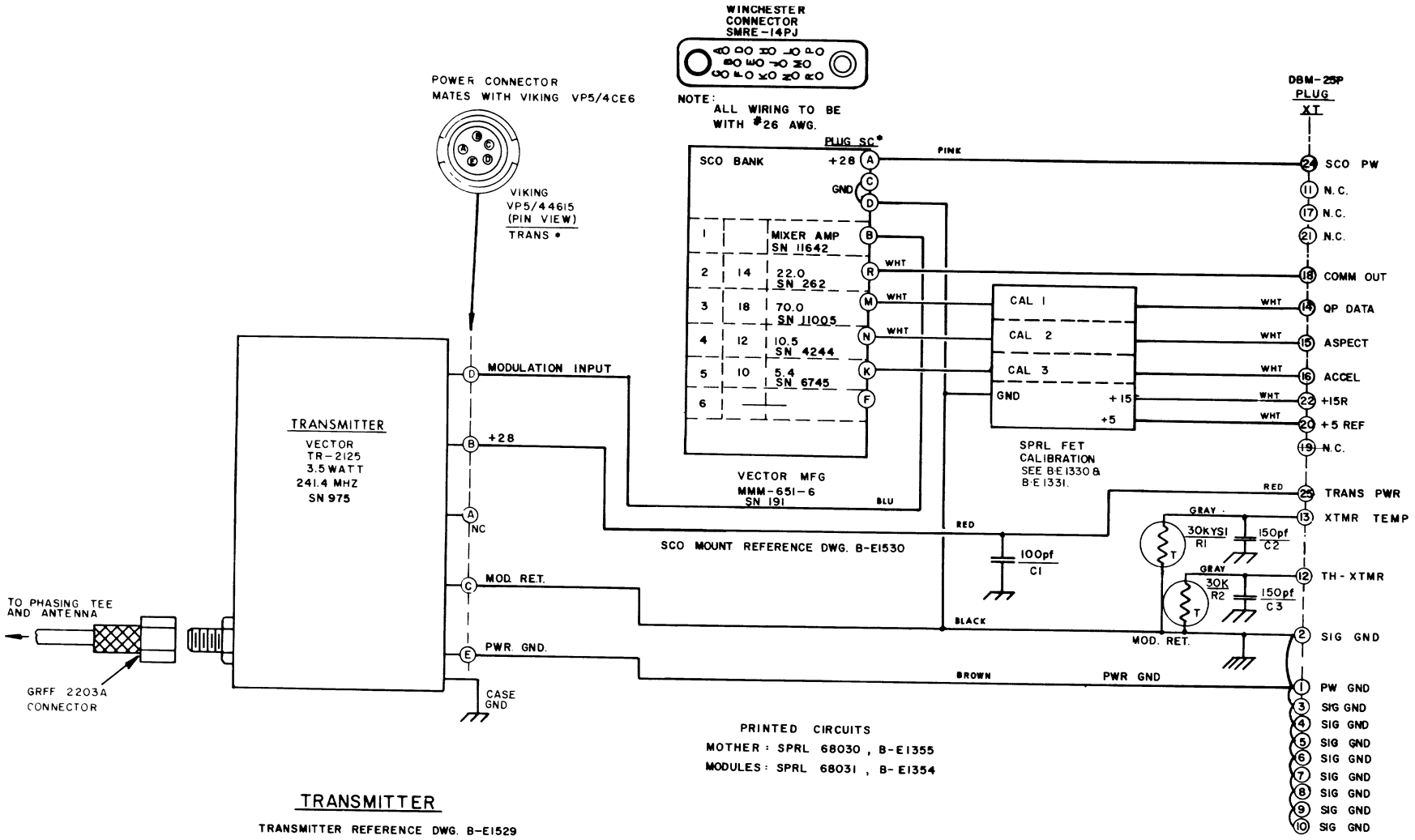

Figure 32. Subcarrier oscillator and transmitter deck interface.

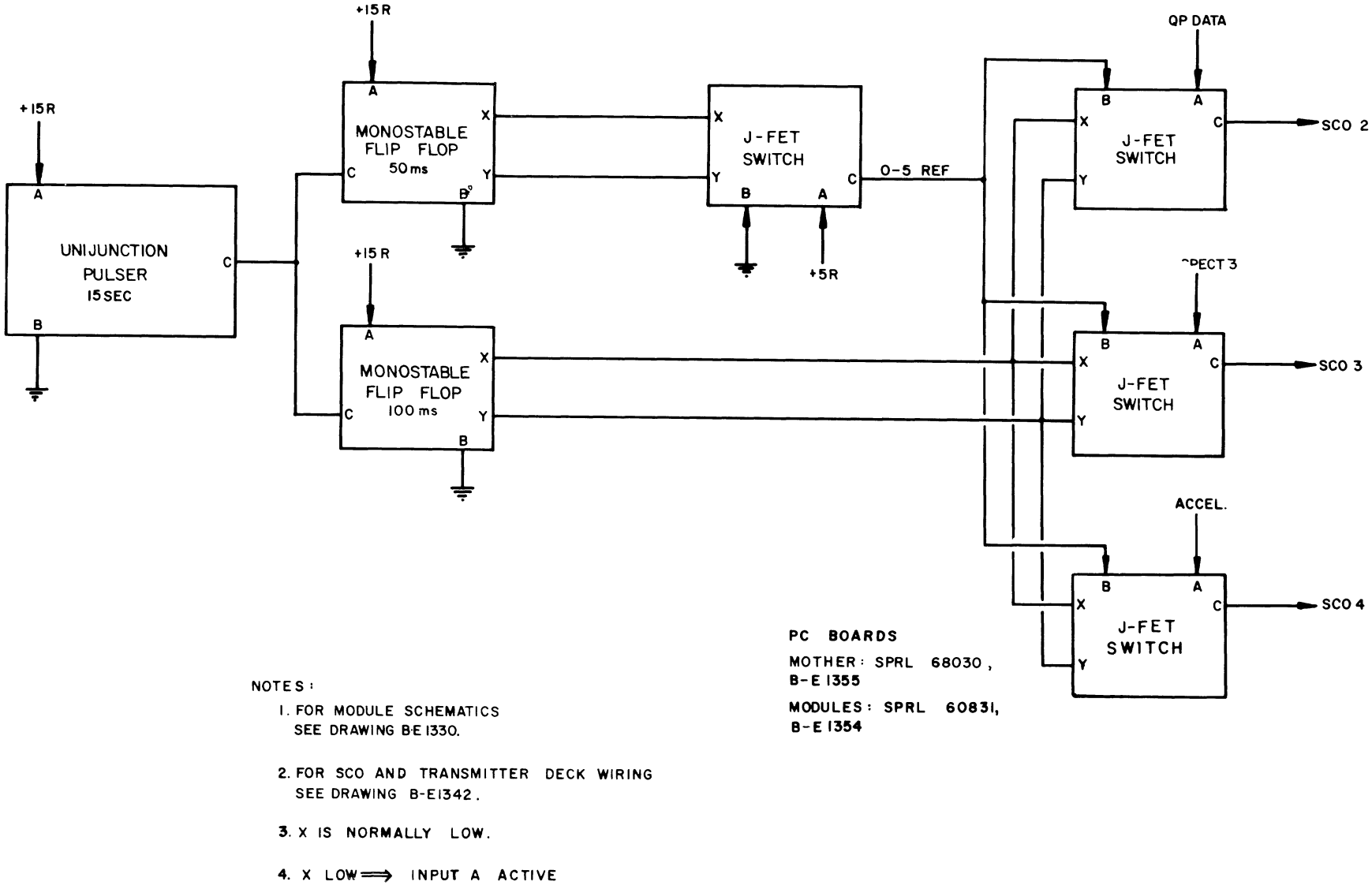

Figure 33. Subcarrier oscillator block diagram.

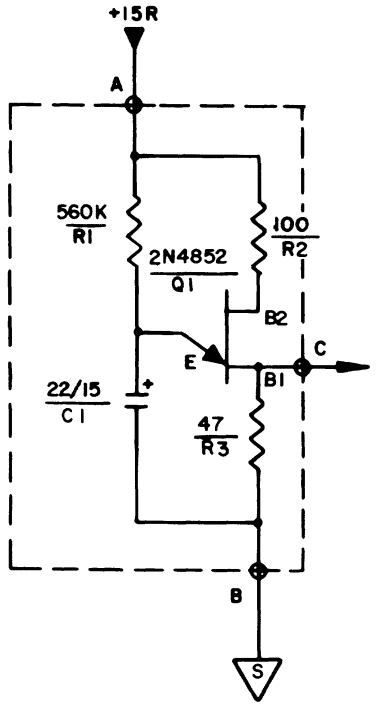

UNIJUNCTION PULSER
15 SECONDS

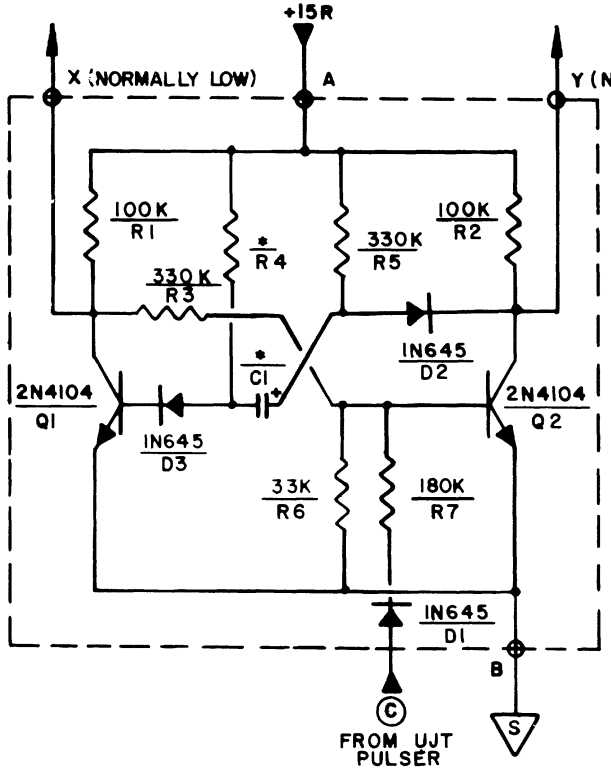

FROM UJT
PULSER

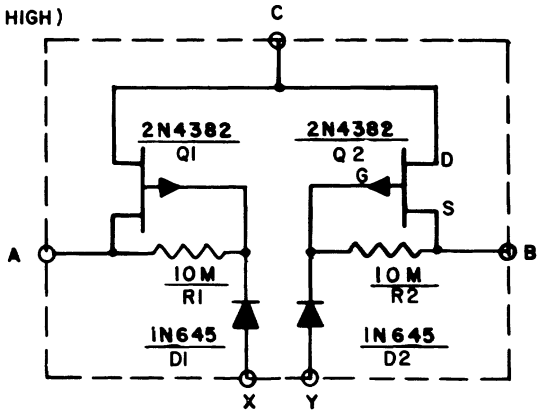

FET SWITCH

X LOW ⟹ INPUT A ACTIVE

MONOSTABLE FLIP FLOP

*	50 ms	100ms
R4	680 K	680 K
C1	.1µf	.2µf

PC BOARD
SPRL 68031, B-E1354

Figure 34. Subcarrier oscillator calibration circuits.

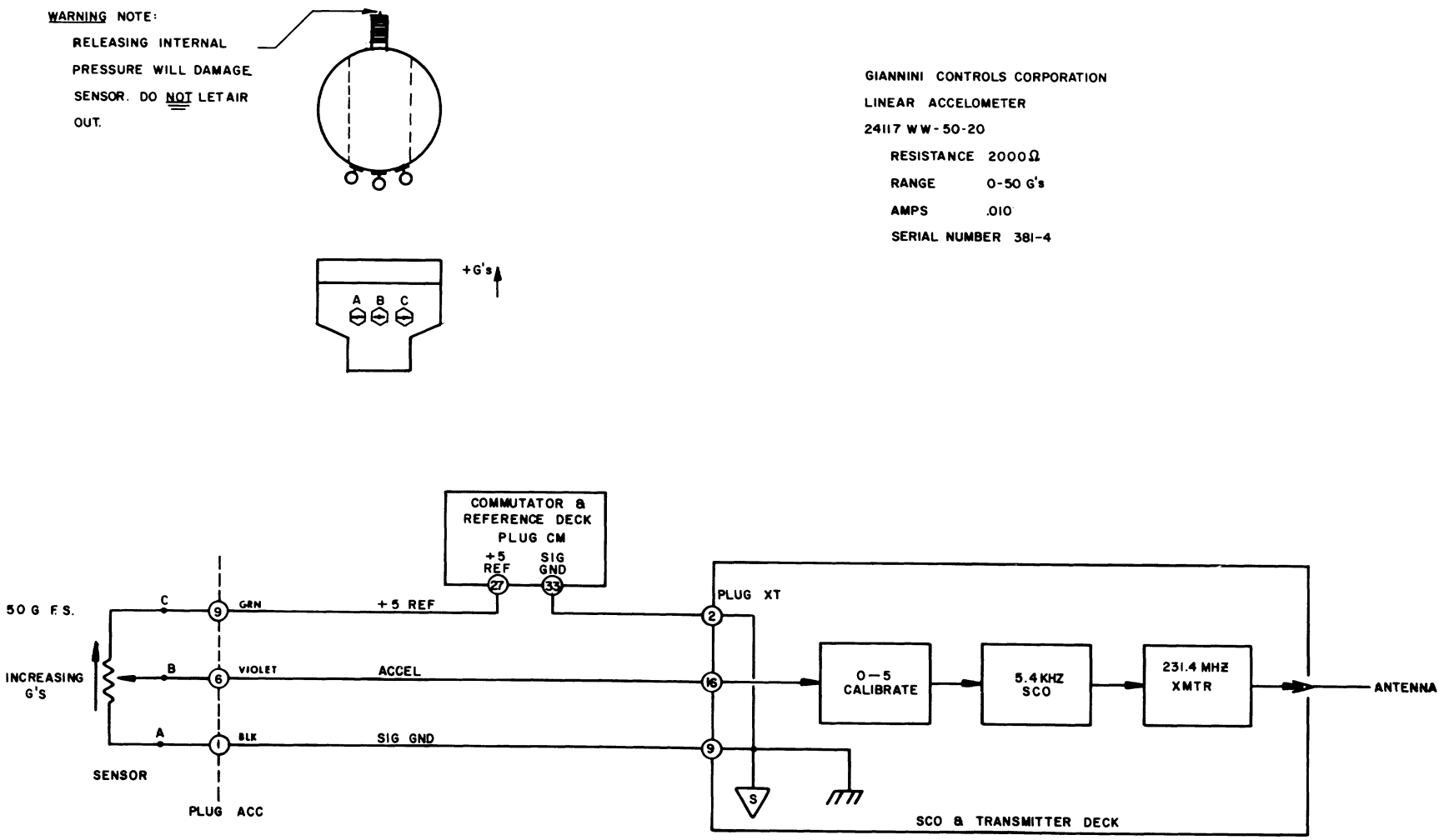

SENSOR INTERFACE 5.000V
SENSOR RESISTANCE 2000 Ω
SENSOR LINEARITY

Figure 35. Accelerometer and interface.

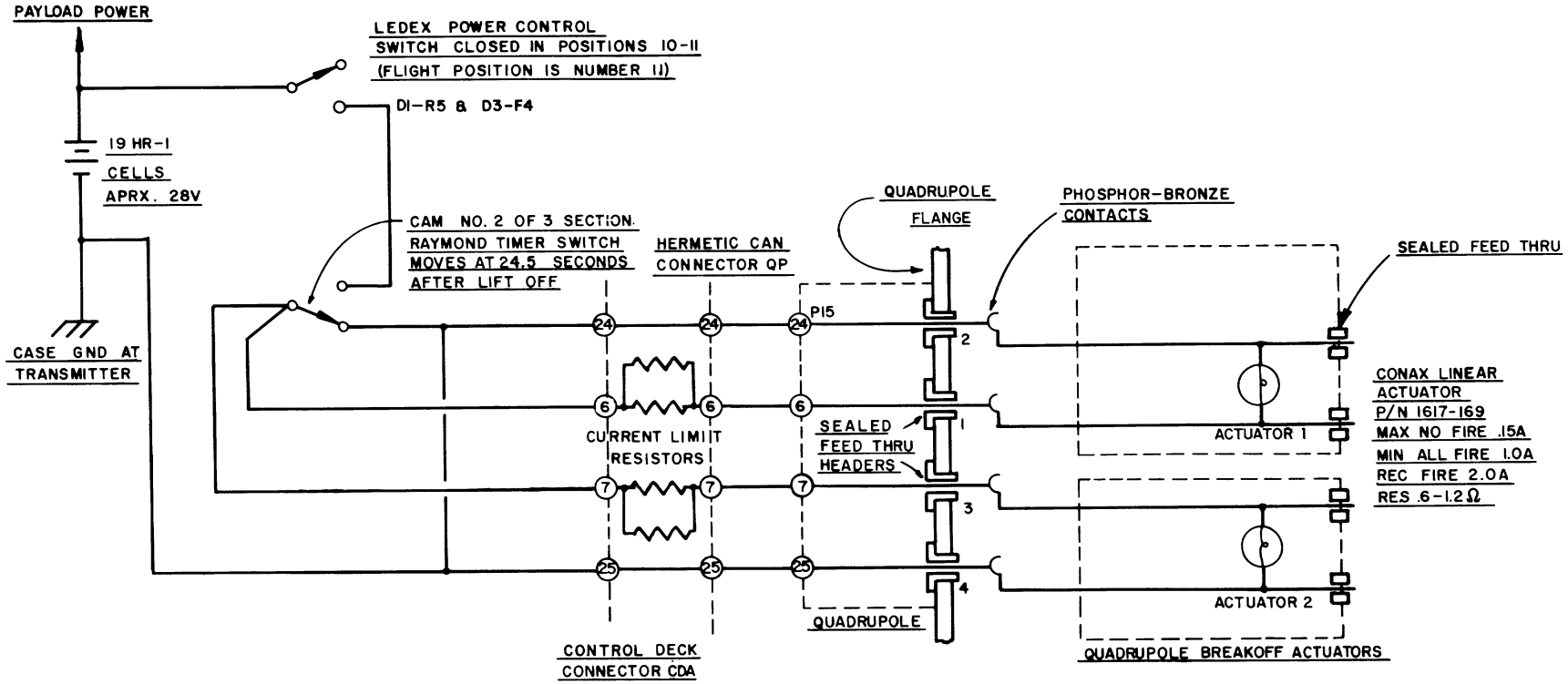

Figure 36. Pyrotechnic firing circuits.

5. DATA

The telemetered data were recorded on both magnetic and paper tapes at the Wallops Island Main Base and Goddard Space Flight Center Station A receiving stations. The mass spectrometer data were reduced from paper records by Goddard Space Flight Center personnel and are not discussed here. The temperature and pressure data were reduced by computer techniques from the magnetic tapes.

5.1. TRAJECTORY AND ASPECT

The angle of attack of the payload was assumed to be less than ±5° throughout the meaningful portion of the flight. This was based on the facts that the payload was not despun, the dynamic unbalance was very low, and the static stability margin was extremely high.

The first 83 sec of trajectory information were obtained from MPS-19 radar data which was fitted and smoothed by computer techniques at Wallops Island. The remaining portion of the trajectory was supplied (also by Wallops Island) in the form of Spandar data. Figure 37 shows the trajectory and the occurrence of significant events during the flight.

5.2. TEMPERATURE

The temperature data were reduced from the decommutated magnetic tapes. Figures 38(a) and 38(b) show the theoretical and measured temperature of the nose cone inlet system versus flight time.

5.3. PRESSURE

The pressure data were reduced from the decommutated magnetic tapes. Figures 39(a) and 39(b) show the theoretical and measured nose cone inlet system temperature versus flight time.

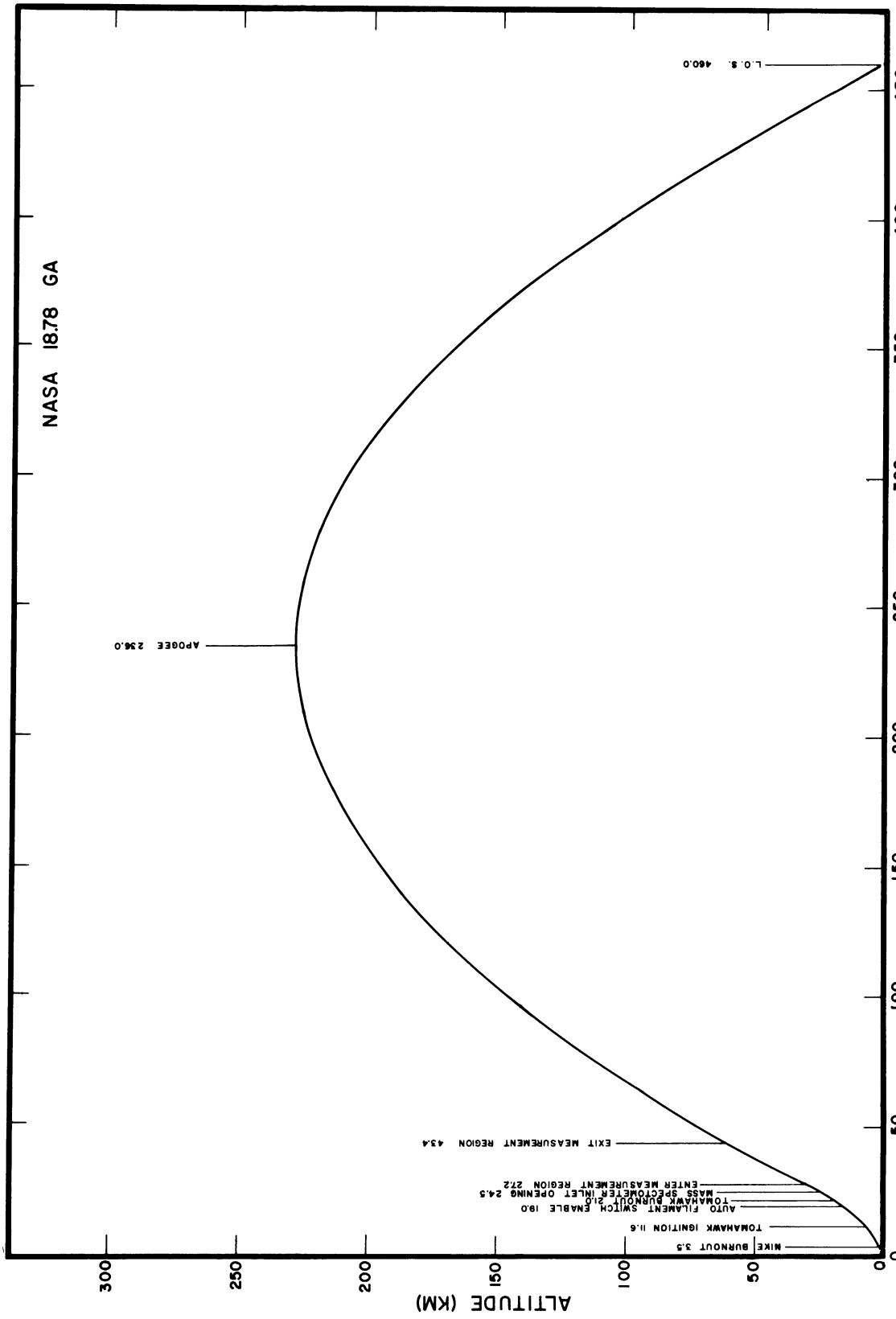

Figure 37. Trajectory.

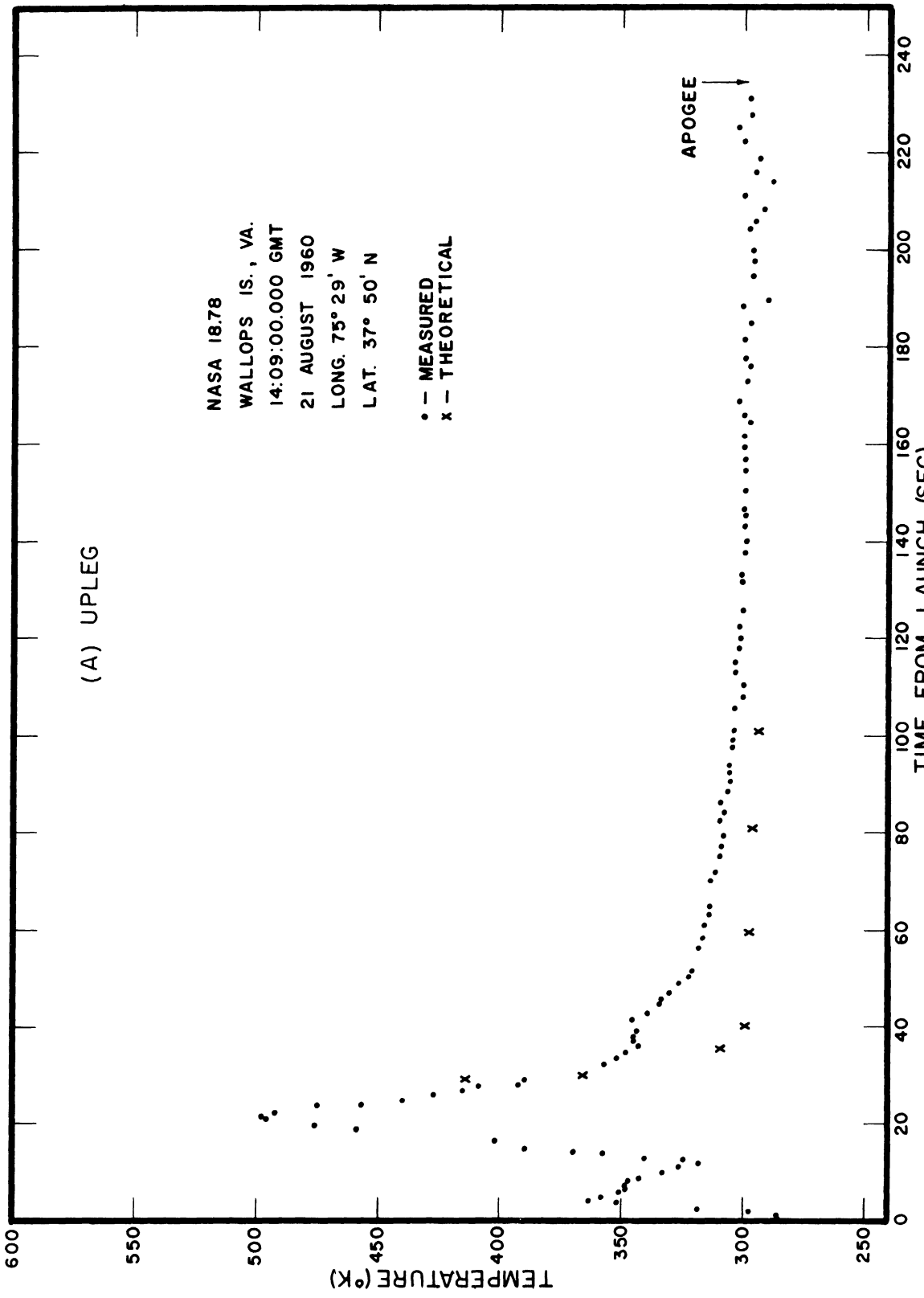

Figure 38. Temperature vs. altitude.

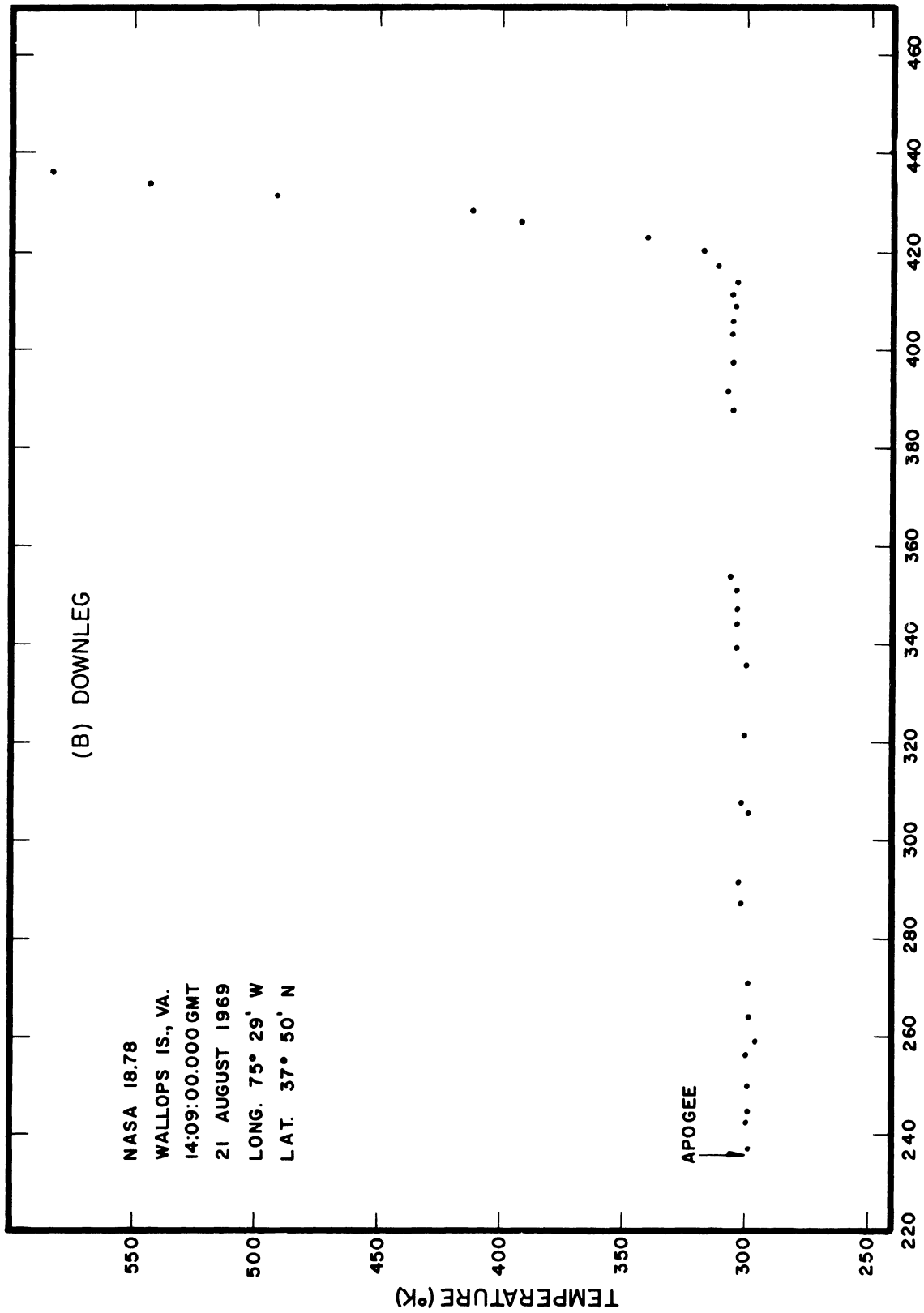

Figure 38. (Concluded).

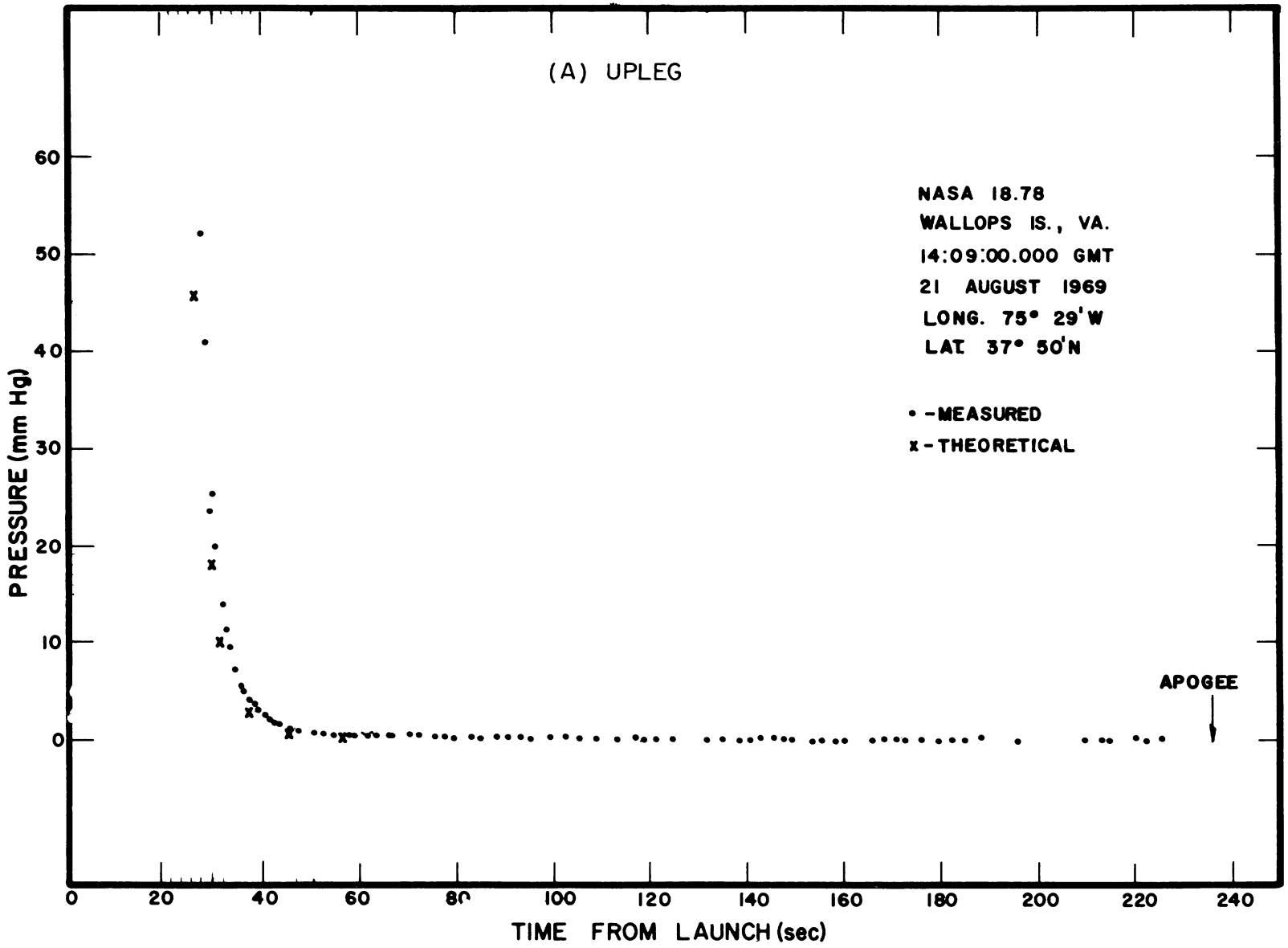

Figure 39. Pressure vs. altitude.

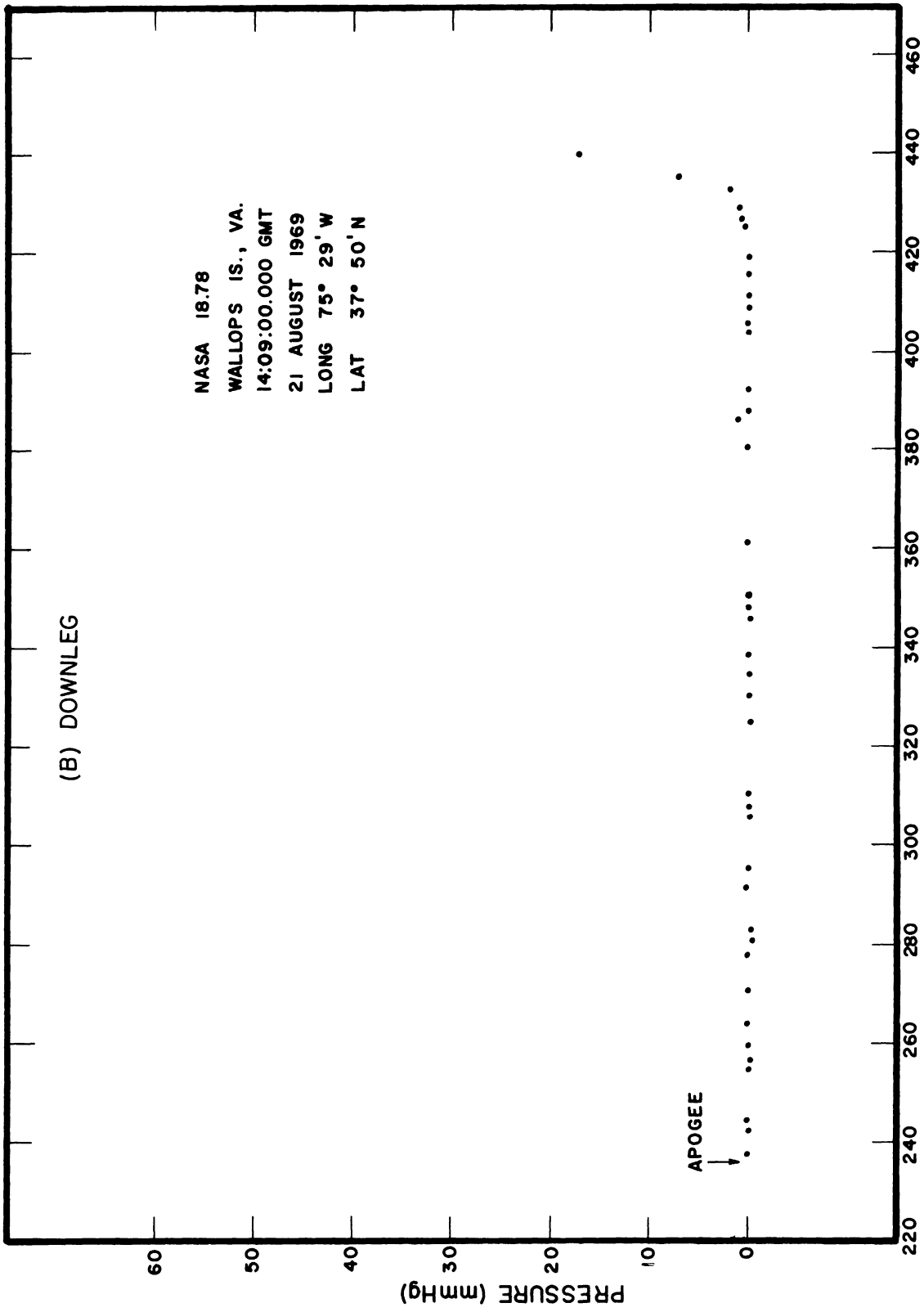

Figure 39. (Concluded).

6. REFERENCES

Consultants and Designers, Inc., Final Report for Planetary Quadrupole Mass Spectrometer (Model A) Electronics, Contract NAS 5-9245, prepared for Goddard Space Flight Center, Greenbelt, Maryland, March 1968.

Kerne, B., J. Deskevich, and W. Elder, Design Review of the Mass Spectrometer, Operations Research, Inc., Technical Report 445, prepared for Goddard Space Flight Center, Greenbelt, Maryland, 8 January 1968.

Simmons, R. W., NASA 18.56 Thermosphere Probe Experiment, The University of Michigan Sounding Rocket Flight Report 07065-11-R, May 1969.

APPENDIX

MODEL TESTS BY GAS DYNAMICS LABORATORIES

A.1. INTRODUCTION

In order to make predictions regarding the air flow rate, pressure, and temperature in a particular air sampling system, it was desirable that a series of model tests be made at conditions somewhat similar to the most severe conditions anticipated for the flight model tube. The most severe conditions of interest here are approximately the following:

Mach number	7.33
Altitude	61,000 ft
Stagnation pressure after normal shock	69 psia
Stagnation temperature	4610°R

It was not practical to simulate these conditions, but it was possible to test a scale model in the Gas Dynamics Laboratories' hypersonic tunnel without excessive effort. This tunnel was designed to operate at a Mach number of 8 with stagnation pressures up to 600 psia and stagnation temperatures up to 1000°F.

A 1/5 scale model was chosen for the tunnel tests since that was considered to be about the maximum size that could be tested without choking the tunnel. Figure 40 is a photograph of this tunnel model. Figures 41, 42, and 43 are drawings of the model.

Although the external dimensions (diameter and length) of the model are 1/5 the corresponding dimensions of the flight nose cone, it was not considered appropriate that the inside diameter of the minimum diameter section of the sampling supply tube should be scaled down by 1/5. A 1/5 scaling factor on the diameter would reduce the minimum passage from 0.040 in. diameter to 0.008 in. diameter. It was considered more meaningful to scale the restricted passage area to 1/5. The length of the restricted passage in the model was chosen so that the L/D ratio would be the same for the model as for the full scale unit. The dimensions of the other sections of the sampling duct were scaled in a roughly similar manner and are not critical in determining flow conditions.

The tunnel model was designed so that the minimum diameter section of the sampling supply duct could be changed easily. Three different inserts were made (see Figure 42), but only the 0.018 in. diameter insert was used in the tests. Further tests did not appear to be warranted at the time.

The four radial exhaust ports in the model were drilled with a No. 25 drill (0.149 in. diameter). This diameter was 1/5 of the exhaust hole diameter in the flight cone; thus, the model exhaust area was 1/25 of the full scale cone. One of the main objectives of the tunnel tests was to determine whether the exhaust ports in the nose cone were properly sized and positioned to exhaust the flow from the sampling system inlet without restricting that flow rate. The use of undersized exhaust ports made the tunnel test results conservative in that if no restriction occurred with the undersized passages, then the correct passage area would provide even less restriction. For example, at the inlet temperatures tested (from 100 to 300°F), it was found that the actual flow rate (through the 0.018 in. diameter by 0.50 in. long insert) was about 60% of the flow rate calculated on the basis of a short choked orifice. It was also found that the downstream pressure needed to be less than about 1/3 of the inlet stagnation pressure in order that the flow rate would not be dependent on the downstream pressure. In other words, if the spectrograph cavity pressures were maintained at less than 1/3 the upstream stagnation pressure, the exhaust ports would not be restricting the sampling flow rate.

Although more extensive tests would have been desirable, it was believed that the test results obtained were adequate to interpret the tunnel test results.

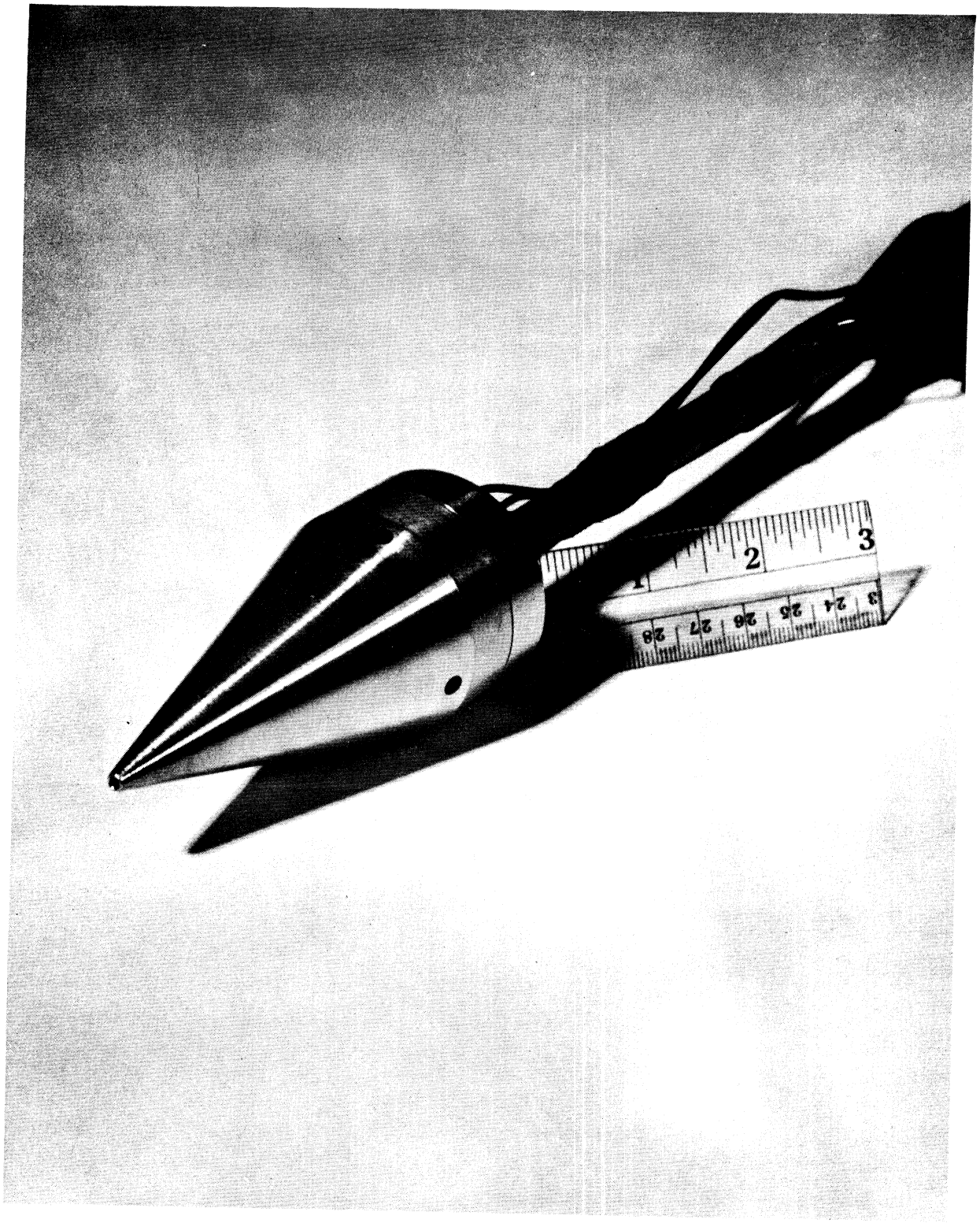

Figure 40. Model for Mach 8 tunnel tests.

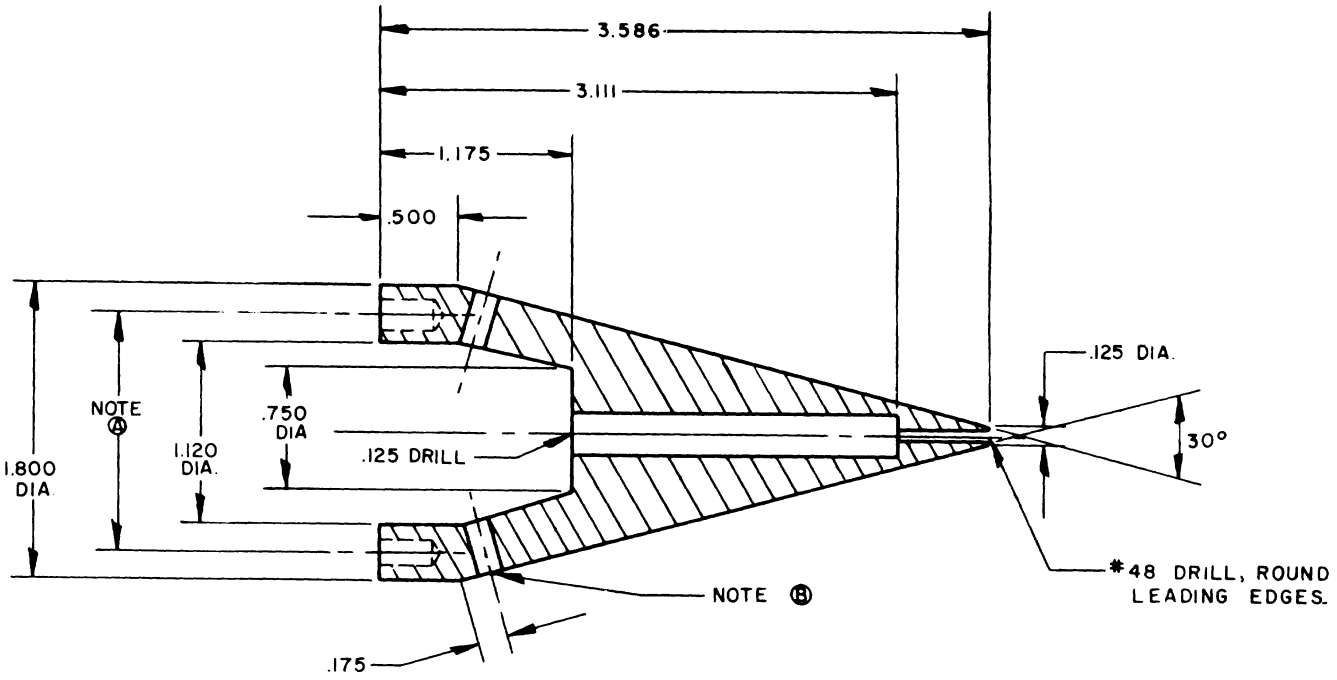

NOTE:

A 1.460 DIA. BOLT CIRCLE DRILL & TAP FOR 6-32 THREAD, .375 DP. 4 HOLES EVENLY SPACED. (90°)

B #25 DRILL NORMAL TO SURFACE OF CONE. 4 HOLES EVENLY SPACED. (90°)

NOSE CONE MODEL
DIMEN. - INCHES
SCALE - FULL
MAT'L. - ALUM
1 REQ.

Figure 41. Wind tunnel model, nose cone.

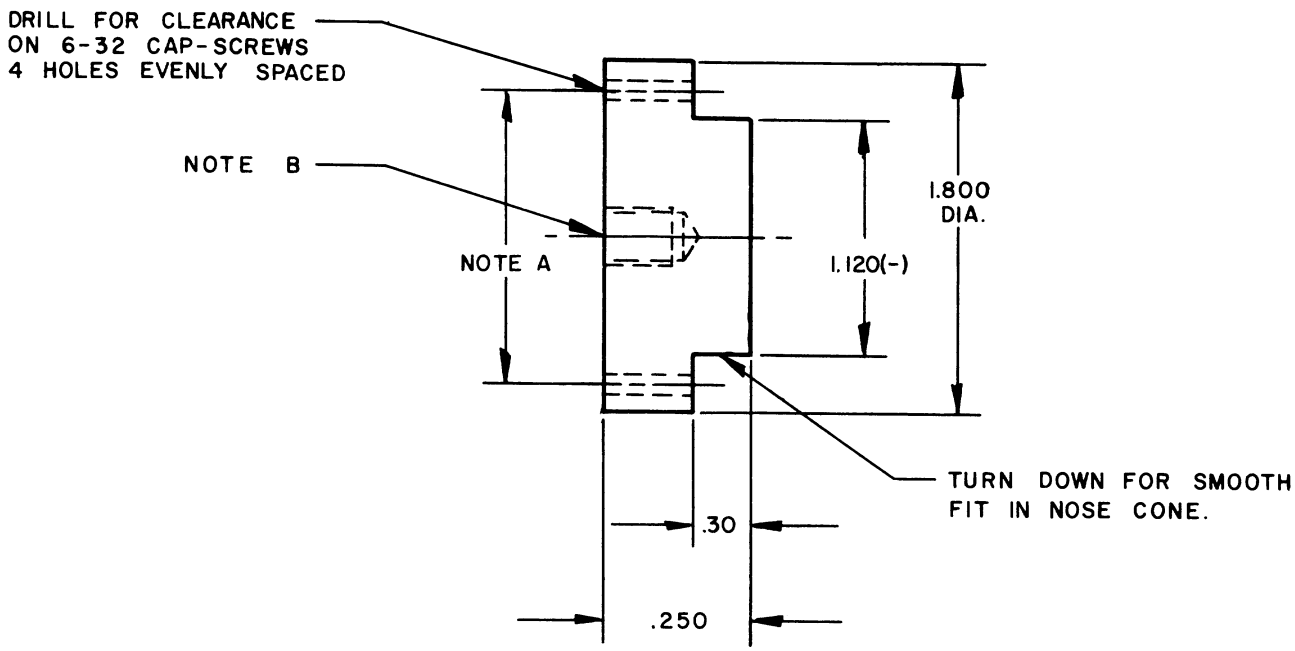

NOTE:

A. MATCH BOLT CIRCLE PATTERN OF NOSE CONE.

B. DRILL & TAP TO MATCH EXISTING THREAD ON MODEL STING. (3/8-24)

NOSE CONE MOUNT
FULL SCALE
MATR. ALUM
2 REQ'D.

Figure 42. Wind tunnel model adapter.

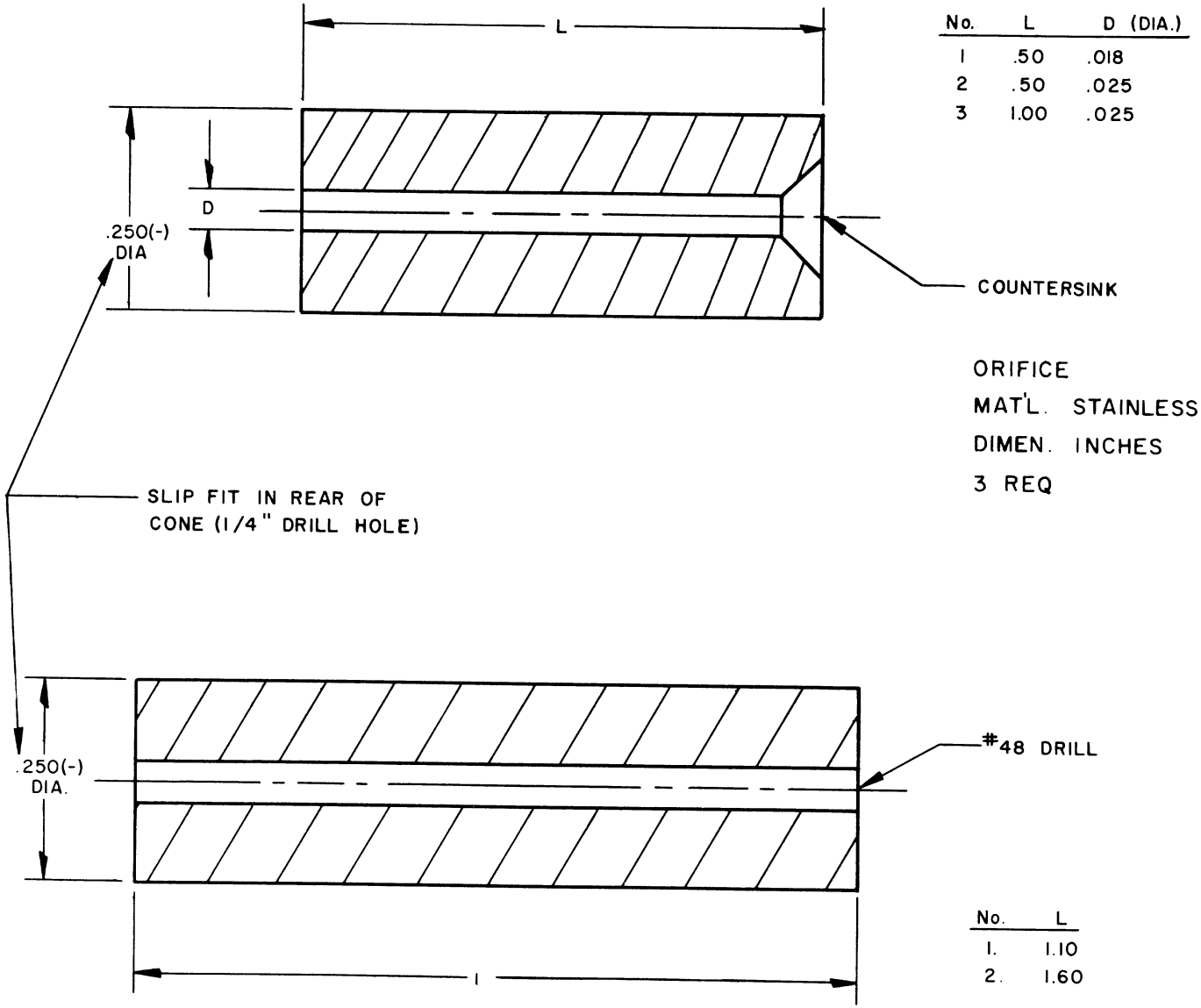

Figure 43. Wind tunnel model, capillary section.

A.2. WIND TUNNEL TESTS

As mentioned previously, a 1/5 scale model of the nose cone was tested in the Mach 8 facility. A major portion of the air sampling passage was duplicated in the nose cone. The sampling system used in the scale model was designed with the capillary section removable. This feature served two purposes: first, any scale effects on the sampling flow rates could be corrected, and second, the effects of capillary size and material (heat transfer rates) could be changed if the sampling system performance was not adequate.

The wind tunnel model was made of aluminum and the capillary sections were made of stainless steel. Although the full scale nose cone sampling system was made of stainless steel, it was felt that the saving in time and machining costs justified an aluminum model. Since the effects of heat transfer on the flow would be controlled by the capillary section, the capillary inserts were made of the same material as the full scale system. The model duplicated the full scale nose cone to a point 2.5 in. back on the cylindrical body. The model terminated there with an adapter plug which mated the nose cone to a tunnel sting. The sting in turn held and positioned the model in the tunnel flow field.

A.3. MODEL INSTRUMENTATION

Provisions were made for monitoring seven pressures and one temperature on the model. Figure 44 indicates the points where pressure measurements were taken. Points 1, 2, 4, and 5 were all static pressure measurements on the surface of the cone, while points 6 and 7 were static pressure measurements on the surface of the cylindrical body joining the cone. Point 3 is the pressure in the nose cone cavity. A temperature measurement of the gas flow into the cavity was also made. An iron-constantan thermocouple was used for the temperature measurement. The cavity is the plenum into which the sampling air flows before venting through the cone surface.

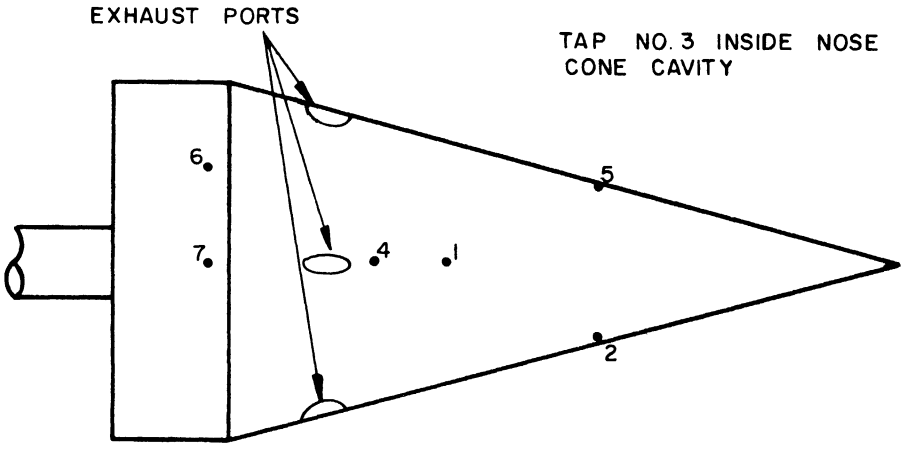

Figure 44. Pressure tap locations.

The pressure measurements were made via a pressure transducer data acquisition system. The output of the transducer is digitized and punched on paper tape. The temperature measurement was recorded on an x-y recorder. The y channel was run in time-base mode giving a recording of temperature versus time.

A.4. TEST PROGRAM

Because of time limitations, only a small number of tests were planned. Also, the information that could be gathered from the model was reduced to one particular aspect of the gas sampling system. The major emphasis was placed on whether the gas sampling system would maintain an adequate flow rate over a given altitude range. In the wind tunnel tests, this constituted the measurement of the cavity pressure level as a function of tunnel total pressure levels.

The tunnel operating conditions were such that a Mach 8 flow could be produced with a total pressure variation between 50 psia and 500 psia, the altitude equivalent being approximately 200,000 to 120,000 ft. It was anticipated that the exhaust ports in the model could be easily enlarged but the test results indicated that it would not be necessary.

The rate of air flow through the sampling inlet duct is determined by the temperature and pressure (and composition) of the air upstream of the minimum diameter section, provided that the pressure in the downstream spectrograph cavity is below a certain critical value. This critical pressure would be about 1/2 of the upstream stagnation pressure if the restricted (throat) section were only a few throat diameters long, but in the case where the restricted section is many diameters long, the critical pressure must generally be somewhat lower. A series of bench model tests were made to determine, at least approximately, the values of this critical pressure for various inlet conditions.

Figure 45 is a drawing of this bench model of the sampling flow inlet duct. This model also was designed to allow for easy changes of the minimum diameter section, but only the 0.018 in. diameter insert was tested. Upstream of this bench model an electrically heated stainless steel tube was used to raise the incoming temperature of the gas. The air flow fed into the bench model was measured by a calibrated capillary tube system. During a test, the flow rate was maintained at a constant value independent of the heat input and the pressure upstream of the test section.

The bench tests were not nearly extensive enough to allow accurate extrapolation to the flight model, but certain approximate values were determined.

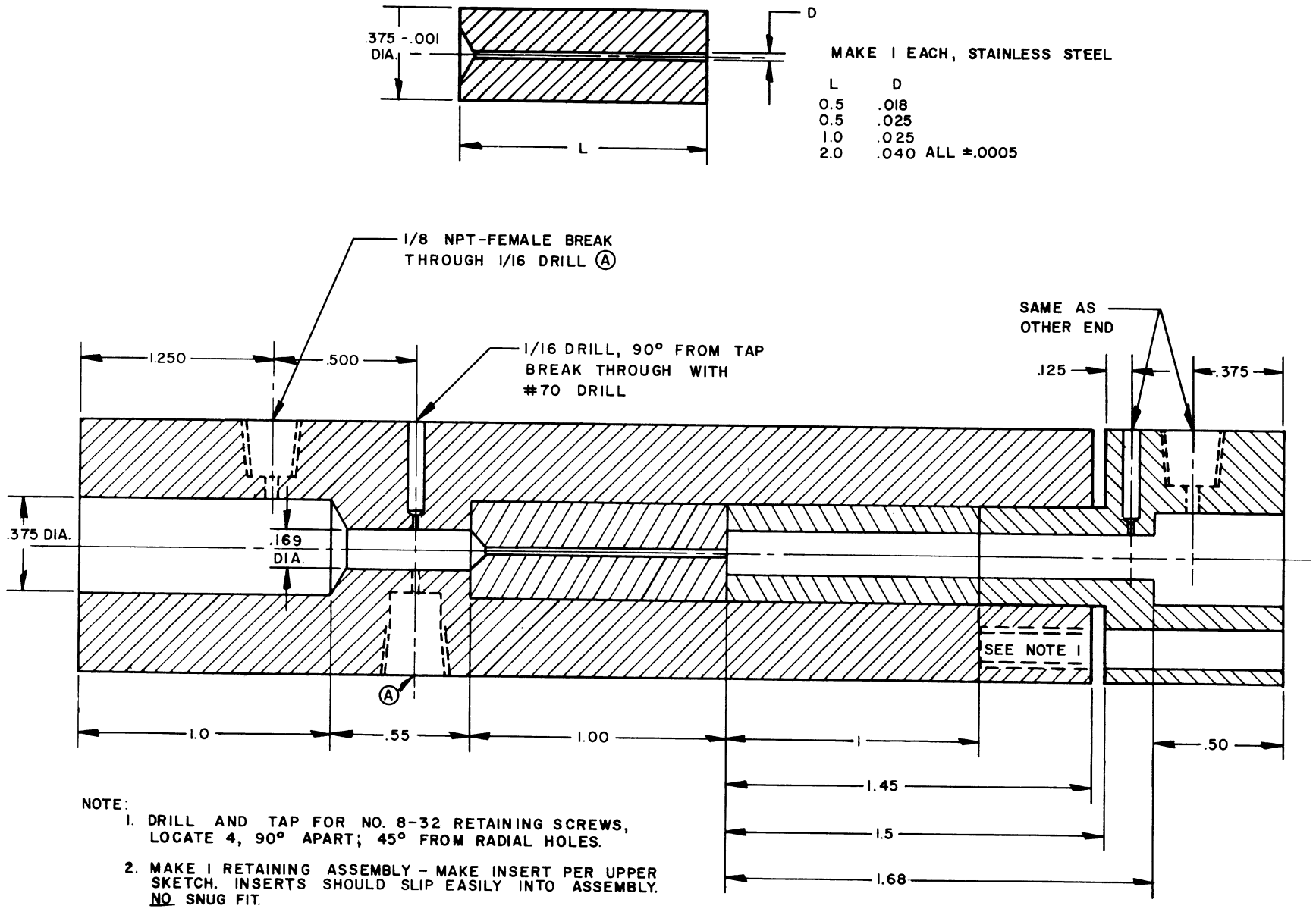

Figure 45. Bench model of sampling flow inlet passage.

A.5. TEST RESULTS

Three series of tests were run. The total pressure for these runs varied from 60 to 390 psia with a flow Mach number of 8.03. Total temperatures for these tests was 760°F. The tunnel operating conditions are listed below. Since the primary emphasis was on the sampling system flow rate, only the data related to this feature were reduced.

A plot of cavity pressure versus equivalent altitude is presented in Figure 46. Also plotted on this figure are the computed values for the pressure on the surface of the cone and the total pressure behind a normal shock. The results indicate that the cavity pressure was slightly higher than the theoretical cone surface pressure, which would necessarily be the case as long as there was flow from the sampling system. Also, the fact that the cavity pressure is roughly 1/6 of the stagnation pressure at the entrance of the sampling system inlet indicates that the flow in the restricted portion of the supply tube was choked.

As mentioned previously, a thermocouple was installed to measure the temperature of flow entering the cone cavity. Preliminary indications were that flow temperatures were about 20% of the free stream total temperature. A Schlieren photograph showing the flow field over the test model is also included (Figure 47). This photograph indicates that the low flow rate from the cavity did not significantly disturb the external flow.

More extensive tests with the tunnel test model could be made, but the results presented here are believed adequate to meet the limited objective which prompted this work.

TEST LOG

Run No.	Tunnel Conditions			
	Total Pressure psia	Total Temp °F	Mach No.	Equivalent ARDC Std. Alt.-Ft.
1	62.85	760	8.03	183,000
2	174.3	760	8.03	155,000
3	391.6	760	8.03	133,000

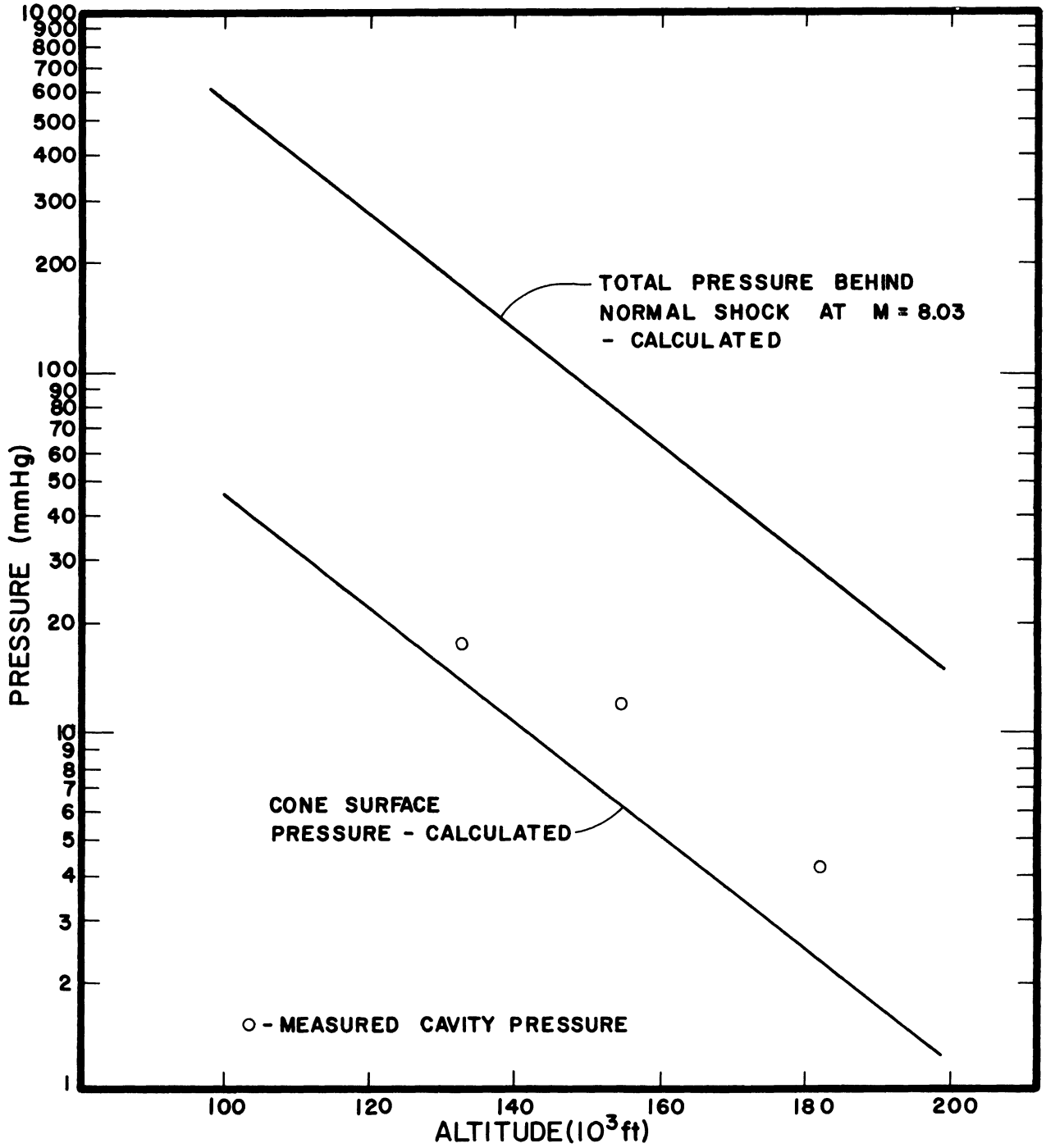

Figure 46. Predicted cavity pressure vs. altitude.

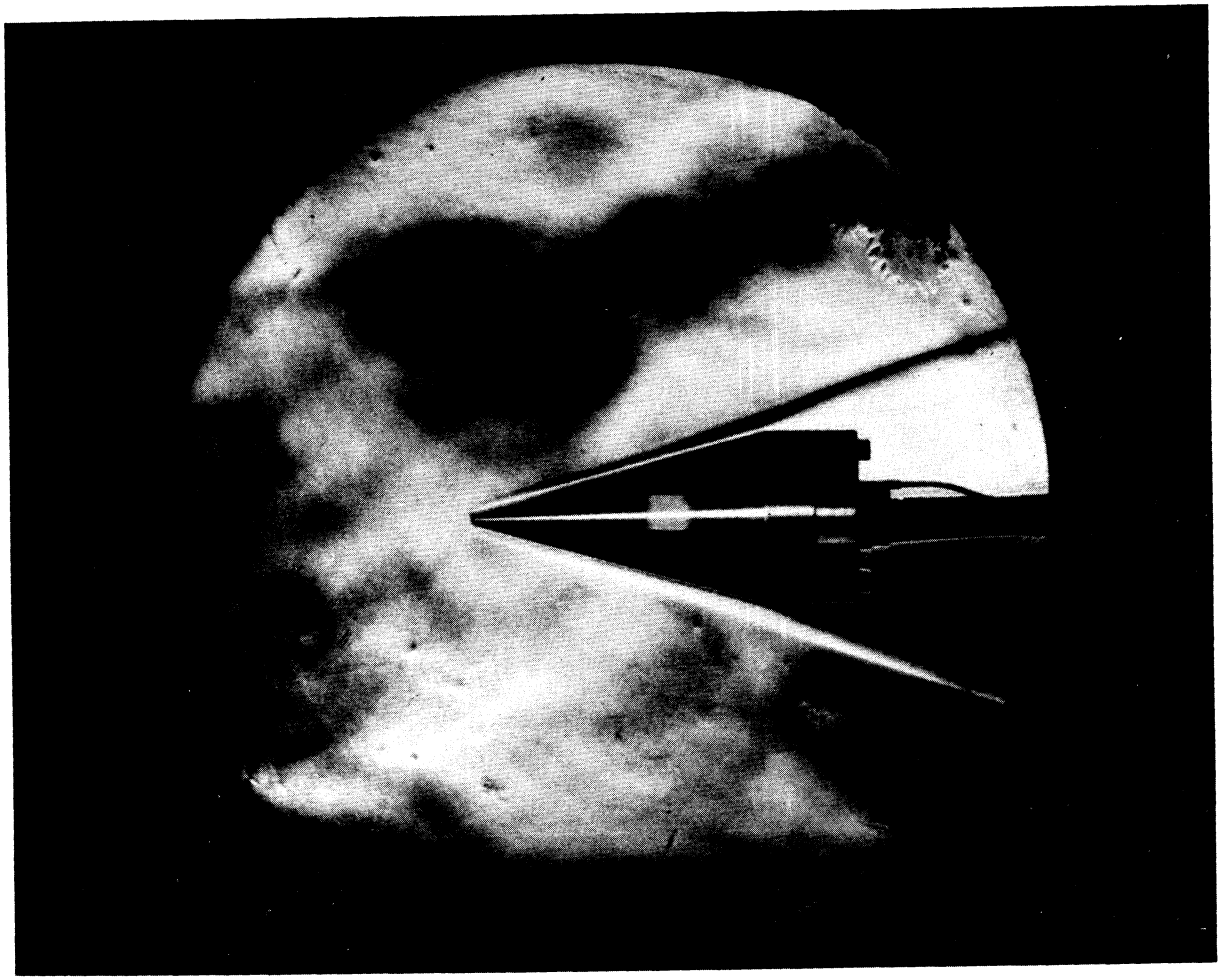

Figure 47. Schlieren photograph of flow field around model in an M = 8.03 stream.